933

INSTITUT DE PHYSIQUE DE L'UNIVERSITE DE NEUCHATEL

TRANSITIONS DE PHASE DU RESEAU DE VORTEX DANS DES COUCHES MINCES SUPRACONDUCTRICES.

Thèse présentée à la Faculté des Sciences de l'Université de Neuchâtel pour l'obtention du grade de docteur ès Sciences

par

NSABIMANA Marcel
Physicien diplômé

mai 1983

IMPRIMATUR POUR LA THÈSE

Transitions de phase du réseau de vortex

dans des couches minces supraconductrices

de M *onsieur Marcel Nsabimana*

UNIVERSITÉ DE NEUCHATEL

FACULTÉ DES SCIENCES

La Faculté des sciences de l'Université de Neuchâtel,
sur le rapport des membres du jury,

MM. les professeurs P. Martinoli, H. Beck

et Ø. Fischer (Genève)

autorise l'impression de la présente thèse.

Neuchâtel, le *14 septembre 1983*

Le doyen:

A. Aeschlimann

Les tirés à part ci-joints représentent l'essentiel de la thèse de doctorat dont le titre et le nom de l'auteur sont repris en page de garde. Le texte complet du manuscrit peut être consulté à la bibliothèque de l'Institut de Physique de l'Université

rue A.-L. Bréguet 1
CH-2000 NEUCHATEL

Helvetica Physica Acta,
Vol. 56 (1983) 765-785

0018-0238/83/010765-21$1.50+0.20/0

SEARCH FOR TWO-DIMENSIONAL MELTING IN A LATTICE OF SUPERCONDUCTING VORTICES

P. Martinoli, M. Nsabimana, G.A. Racine and H. Beck

Institut de Physique, Université de Neuchâtel,
CH - 2000 Neuchâtel, Switzerland

and

J.R. Clem

AMES Laboratory-USDOE and Department of Physics,
Iowa State University, Ames, Iowa 50011, USA

ABSTRACT : The dynamic shear response Z of the vortex lattice in superconducting granular Al films shows interesting features near T_M, the Kosterlitz-Thouless temperature for dislocation-mediated melting. The T-dependence of Z is interpreted in terms of the coupled motion of displacement field and dislocations in an elastic continuum. Pinning of the vortices by inhomogeneities seems to play an important role.

I. INTRODUCTION

It has been proposed [1,2] that a lattice of quantized vortices in thin superconducting films can be considered as a two-dimensional (2D) crystal undergoing a transition from a solid-like to a fluid-like phase at a melting temperature T_M determined by the Kosterlitz-Thouless [3] criterion for the existence of topological order in two dimensions. According to this theory, the mechanism driving the melting transition is believed to be the unbinding of bound pairs of dislocations, which, together with phonons, represent the thermal excitations of a 2D crystal. For an incompressible 2D crystal, as it is the case for a lattice of superconducting vortices, the melting temperature T_M is given by the following implicit relation [3] :

$$4\pi K_B T_M = \mu_R(T_M^-) a^2 \quad , \tag{1}$$

where a is the lattice parameter and $\mu_R(T_M^-)$ the effective shear modulus of the crystal at the phase transition as T_M is approached from the solid phase. In the static case ($\omega = 0$) μ_R jumps discontinuously to zero at T_M and vanishes in the liquid phase. Expressing μ_R in terms of superconducting parameters, Fisher [2] has shown that for a lattice of vortices Eq. (1) can be written in the form :

$$\frac{T_M}{T_c} = 1 - \frac{3.8}{A_1} \frac{R_{n\square}}{R_u} \quad , \tag{2}$$

an expression showing that the melting transition should occur always below T_c, the BCS superconducting transition temperature. In Eq. (2) $R_{n\square}$ is the normal-state sheet resistance of the superconducting film, R_u the universal resistance $\hbar/e^2$ and A_1 is a constant, which lies between 0.4 and 0.75, accounting for the renormalization of the shear modulus.

Recently, Fiory and Hebard [4] provided clear evidence for melting phenomena occurring in a 2D lattice of superconducting vortices. However, since vortex pinning was not explicitly included in their analysis, they were unable to ascertain whether the observed transition was driven by the unbinding of dislocation dipoles as predicted by detailed theories [5,6] of 2D melting.

In this paper, we report a study of the ac complex impedance of superconducting Al-films mounted in the so-called Corbino-disk geometry [7]. In this particular configuration the oscillating driving Lorentz force acting on the vortices, which results from an ac current flowing radially in the superconducting disk, couples only to shear deformations of the vortex medium. As a consequence, it was originally thought that this experiment was ideally suited to provide important insight into the unique dynamical aspects of dislocation-mediated melting.

The experimental results described in Section II are indeed consistent with the hypothesis of vortex-lattice melting. A detailed analysis of the data, however, shows that vortex pinning, as in Fiory-Hebard's experiments, plays an essential role in determining the dynamic response of the vortex medium in both the solid and fluid phase. In Section III, therefore, we develop a model which explicitly incorporates pinning phenomena in the dynamics of an elastic vortex continuum with dislocations. The model qualitatively explains the essential features of our data and brings new insight into the role of pinning in melting phenomena of a lattice of superconducting vortices.

II. EXPERIMENTAL RESULTS

To realize the desired radial current-density distribution characterizing the Corbino-disk geometry, granular Al-films of circular shape were mounted in a coaxial current-feeding configuration. Electrical contacts were obtained by pressing against the film surface the indium tip of the central electrode and an indium O-ring which acts as outer circular electrode. In order to allow free access of magnetic flux to the film region, the external superconducting In-electrode was interrupted over a very short portion of its circular path. The diameter, $2R_i$, of the central contact is of the order of 1 mm, whereas the corresponding dimension, $2R_o$, of the external electrode is 18 mm. The ac complex impedance Z of the superconducting film was inferred from $V = ZI$, where I is the constant rms value of the driving ac current and V the rms value of the ac potential difference between the central and the outer electrode measured with a conventional phase-sensitive detector. I never exceeded ~ 1 μA, a value resulting in a maximum current density of the order of ~ 1 A/cm^2 in the immediate vicinity of the central electrode. Typically, at these current levels the sensitivity of the detector allowed to measure impedances of the order of a few mΩ. The

frequency range covered by the experiments reported in this paper extends from 100 Hz up to 100 kHz. At low frequencies (less than ~ 5 kHz) the correct phase setting was obtained by adjusting the phase shift of the detector to null the signal from the film well above its transition temperature (at T = 4.2 K). This corresponds to the 90° phase setting used to measure the quadrature or imaginary part of Z (Im[Z]). At high frequencies, where spurious inductive pick-up from the measuring circuit was not negligible, a more elaborated procedure was used.

According to Hebard and Fiory [8], the complex impedance Z of a 2D superconductor can be written in the form :

$$Z = i\omega L_K + Z_v \ , \tag{3}$$

an expression stating that Z is the series connection of the inductive contribution, ωL_K, due to the superfluid background, and of the impedance Z_v arising from superconducting vortices. Estimates of the kinetic inductance $L_K = (1/2)\mu_o \Lambda \ell n(R_o/R_i)$, where Λ is the effective penetration depth in thin superconducting films, using typical parameters for our Al-films show that ωL_K, in the temperature region of interest, is always well below the sensitivity of our detector. Thus, except very near T_c, where ωL_K, being inversely proportional to the superfluid density which diverges as $[1 - (T/T_c)]^{-1}$, makes the dominant contribution to Z, what we actuelly measure in our experiments is the complex vortex impedance Z_v .

In Figs. 1 and 2 we show experimental results, at B = 5 Gauss, for an Al-film (Al*1*) having $R_{n\square} = 70\ \Omega$. Other parameters of Al*1* are $T_c \simeq 2.04$ K and $d \simeq 100$ Å. We observe a rapid increase in dissipation (Fig. 1) which sets in at a temperature lying within the "melting range" predicted by Eq. (2) ($1.71 \lesssim T_M \lesssim 1.86$ K). Since our method is not sufficiently sensitive to detect the presumably very small dissipative component Re[Z] in what is believed to be a pinned solid vortex

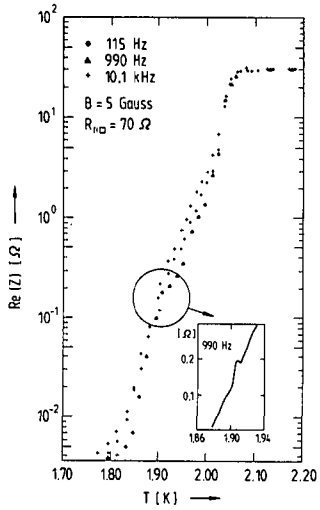

Fig. 1 : Temperature dependence of the real part of the ac complex impedance of Al1.

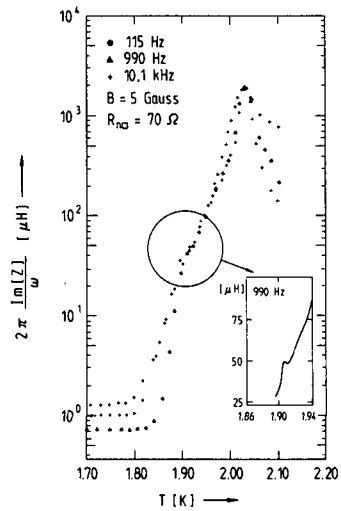

Fig. 2 : Temperature dependence of the imaginary part of the ac complex impedance of Al1.

phase, we are not able to ascertain whether Re[Z] exhibits, near T_M, the break in slope observed by Fiory and Hebard [4] using a different technique. Closer inspection of Fig. 1 shows an additional feature of the data, namely a slight change in slope around 1.9 K which for the results at 990 Hz is associated with the appearance of the small peak shown in the insert. Above 1.9 K Re[Z] is essentially independent of ω in the explored frequency range and exhibit a thermally activated behaviour. The inductive component Im[Z] of Al1 (Fig. 2) shows a definite break in slope at about 1.8 K. Below this temperature, Im[Z] is certainly larger than Re[Z], an indication that pinning effects play a major role in determining the dynamic response of what is presumably the solid-like vortex phase. Above 1.8 K, however, there is a crossover to a régime where Im[Z] is less than Re[Z], a feature consistent with the motion of uncorrelated vortices interacting as individual "particles" with the structural

inhomogeneities responsible for vortex pinning (see Section III c). Im[Z] also shows a little peak structure at about 1.9 K in the data taken at 990 Hz and a weak change in slope at the other frequencies. Above 1.9 K there is again evidence for thermally activated vortex motion and Im[Z] is proportional to ω at low frequencies. On the high temperature side the data of Fig. 2 culminate in a well defined peak at 2.03 K which is related to the smoothed divergence of L_K at the superconducting - normal state transition.

Peak structures and changes in slope above T_M are very pronounced in the data for Al2 (Fig. 3, 4 and 5), a granular Al-film having the same $R_{n\square}$ as Al1, $T_c \approx 2.27$ K, d ≈ 200 Å and for which T_M lies in the 1.90 - 2.07 K range. As shown by Fig. 4 and 5, the position and strength of the peaks are practically independent of frequency. Their intensity, however, depends, even at the lowest excitation levels used in our experiments, on the amplitude of the driving ac current. Moreover, the dissipation associated with the peak in Re[Z] is much larger than what one calculates for free vortex motion from the Bardeen-Stephen theory [9]. Both features provide a clear indication for a non-linear dynamic response of the vortex medium, presumably due to the presence of strong vortex pinning in Al2. This conjecture is consistent with the observation of a remarkable difference in the shape of the current-voltage characteristics of Al1 and Al2.

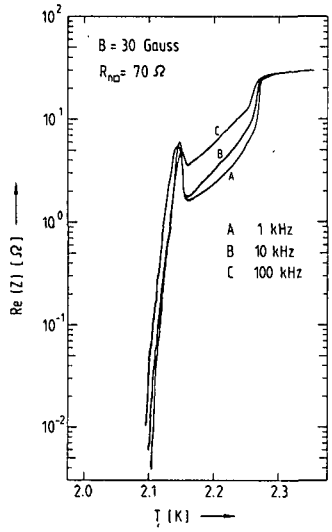

Fig. 3 : Temperature dependence of the real part of the ac complex impedance of Al2. The amplitude of the driving ac current is 1 μA .

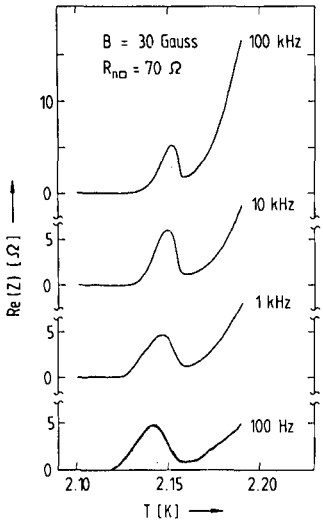

Fig. 4 : Detail of the peak structures of Fig. 3 shown on a linear plot.

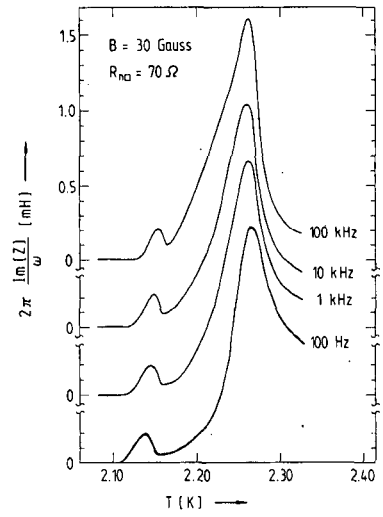

Fig. 5 : Temperature dependance of the imaginary part of the ac complex impedance of Al2 shown on a linear plot. The driving current is the same as in Fig. 3.

Well above T_M, the I-V-curves of both films show a thermally activated behaviour with vanishing critical current at low currents and a linear flux-flow régime at high currents. Below T_M both films have a finite critical current but, while Al1 enters the flux-flow régime with a gradual transition, Al2 shows, at $I = I_c$, a sudden voltage jump after which the film is in the flux-flow state. This feature is interpreted as a manifestation of the existence of very strong pinning centers whose effect is superposed to the usual weak vortex pinning due to the granular nature of the Al-films. Inspection of the structure of our films has, in fact, revealed the presence of holes, presumably resulting from imperfect nucleation, and whose concentration is particularly high for Al2. Holes are known to act as very efficient pinning centers [10]. It is clear, therefore, that a careful analysis of the experimental results reported in this

Section must also take into account phenomena associated with strong vortex pinning.

III. THEORETICAL CONSIDERATIONS

A. 2D Vortex Lattice Without Pinning

In the following discussion the lattice of quantized superconducting vortices is considered as a 2D elastic continuum where thermally excited dislocations form a system of "vector charges" with properties similar to those of a 2D Coulomb gas [3,11]. Since it is energetically more favourable to create pairs of dislocations $(\vec{b}, -\vec{b})$ with opposite Burgers vectors, the total Burgers vector charge of the dislocations vanishes. As a consequence, there is no macroscopic bending in the 2D crystal, a condition equivalent to that of overall electroneutrality in the 2D Coulomb gas analogue.

The equation of motion for the total displacement field $\vec{u}$ of the vortex medium can be written in the form [12] :

$$\eta \frac{\partial u_i}{\partial t} = \frac{\partial \sigma_{ik}}{\partial x_k} + F_i \ , \tag{4}$$

where the three terms represent, successively, the viscous damping force, the elastic restoring force in presence of dislocations and the external driving force acting (per unit surface) on the 2D vortex medium. The viscosity coefficient η is given by $\eta = B^2/R_{f\square}$, where $R_{f\square}$ is the flux-flow sheet resistance. Since there is no macroscopic bending in the 2D vortex crystal, the stress tensor σ_{ik}, which is related by Hooke's law to the elastic part of the total strain tensor, can be expressed as :

$$\sigma_{ik} = C_{ik\ell m}\left(\frac{\partial u_m}{\partial x_\ell} - P_{\ell m}\right) \ , \tag{5}$$

where $P_{\ell m}$ is the plastic part of the total strain tensor, the so-called dislocation polarization tensor, describing the strain field due to the dislocations. For an isotropic continuum the

tensor of the elastic moduli $C_{ik\ell m}$ is given by :

$$C_{ik\ell m} = \lambda \delta_{ik}\delta_{\ell m} + \mu(\delta_{i\ell}\delta_{km} + \delta_{im}\delta_{k\ell}) \ , \tag{6}$$

where λ and μ are Lamé's coefficients. In particular, μ is the shear modulus of the vortex continuum without dislocations.

In order to discuss effects arising from the presence of thermally excited dislocations, it is convenient to rely again on the 2D Coulomb gas analogue. With this in mind it is quite natural to describe the response of the dislocations to the stress σ_{ik} by means of a susceptibility $\chi_{ik\ell m}(\omega)$ defined by the relation :

$$\tilde{P}_{ik}(\omega) = \chi_{ik\ell m}(\omega)\tilde{\sigma}_{\ell m}(\omega) \ , \tag{7}$$

where the sign "~" denotes the Fourier transform of the corresponding physical quantity. In writing Eq. (7) we have implicitly assumed that the stress field varies slowly over distances of the order of the diffusion length traveled by a dislocation during one cycle [6]. Accordingly, the stress field generated in the vortex medium in response to the external driving force is effectively perceived as a uniform stress by the dislocations. Thus, one can approximate $\chi_{ik\ell m}(\vec{q};\omega)$ by its value, $\chi_{ik\ell m}(\omega)$, at $\vec{q} = 0$.

Considering the vortex lattice as an incompressible continuum, from Eqs. (4), (5), (6) and (7), we obtain :

$$-i\eta\omega\vec{u} = \mu_R(\omega)\Delta\vec{u} + \vec{F} \ . \tag{8}$$

This is the conventional equation of motion for a dissipative elastic medium driven by an oscillating external force. In our approach effects arising from the thermally generated dislocations are incorporated in an effective (or renormalized) shear modulus

$$\mu_R(\omega) = \frac{\mu}{\varepsilon(\omega)} \ , \tag{9}$$

where $\varepsilon(\omega) = 1 + 2\mu\chi(\omega)$ is a dielectric constant accounting for screening of the stress field by the dislocations. $\varepsilon(\omega)$ has been calculated by Ambegoakar et al. [11] in connection with the dynamical response of the 2D Coulomb gas and more recently by Zippelius et al. [6] in a detailed dynamical theory of dislocation-mediated 2D melting. It can be written in the form :

$$\varepsilon(\omega) = \varepsilon_b(\omega) + i2\mu \frac{\sigma}{\omega} , \tag{10}$$

showing that $\varepsilon(\omega)$ is the sum of two contributions. The first one, $\varepsilon_b(\omega)$, which is complex, is due to the motion of bound pairs of dislocations (dislocation dipoles) in response to the oscillating stress field. The second one is associated with free dislocation charges. It vanishes below T_M but makes the dominant contribution to $\varepsilon(\omega)$ above T_M. The analogy with the 2D Coulomb gas allows us to write down immediately the expression for the conductivity σ entering this second term :

$$\sigma = b^2 \frac{D}{k_B T} n_f , \tag{11}$$

where D/k_BT and n_f are, respectively, the mobility and the density of the free dislocations. n_f, in turn, is approximately given by $n_f \approx \xi_+^{-2}(T)$, where $\xi_+(T)$ is the correlation length in the fluid vortex phase ($T > T_M$) [5] :

$$\xi_+(T) \approx a \exp\left[\frac{2\pi}{s}\left(\frac{T}{T_M} - 1\right)^{-\nu}\right] , \tag{12}$$

where $\nu \approx 0{,}37$ for a triangular lattice and s is a non-universal constant.

From Eq. (8) we can now deduce the complex vortex impedance Z_v of the Corbino-disk geometry. In this configuration one is dealing with an azimuthal driving force of the form $\vec{F} = (BI/2\pi r)\hat{e}_\phi$. As a consequence, only shear deformations propagating in the radial direction are excited. Then, a simple calculation shows that :

$$Z_v = \frac{R_{fa}}{2\pi} \int_0^\infty C(q)\left[1 + \frac{i}{\omega\tau_q}\right]^{-1} dq \qquad (13)$$

where $C(q) \approx q^{-1}$ for $R_o^{-1} < q < R_i^{-1}$ and $C(q) \approx 0$ otherwise. In Eq. (13) τ^{-1} is the (complex) relaxation rate of the transverse mode $\vec{q}$ in the dissipative vortex medium :

$$\tau_q^{-1} = \frac{\mu R}{\eta} q^2 = \frac{\mu}{\eta\varepsilon(\omega)} q^2 \ . \qquad (14)$$

Since $\mathrm{Re}[\varepsilon^{-1}(\omega)]$ and $\mathrm{Im}[\varepsilon^{-1}(\omega)]$ show, respectively, a shoulder and a peak at a temperature $T(\omega) \gtrsim T_M$ determined by the condition $\xi^2[T(\omega)] \approx D/\omega$ [11,13], one would expect characteristic structures in Z_v associated with the melting transition of the vortex lattice. Closer inspection of Eq. (13) shows, however, that, at $T = 0$, the relaxation times τ_q of the relevant shear modes consistent with the above form of $C(q)$ lie between $\sim 5 \times 10^{-3}$ s and ~ 1 s for a typical choice of parameters and are even much longer in the vicinity of T_M. In the temperature region of interest $\omega\tau_q$ is therefore much larger than unity at the frequencies used in our experiments. As it clearly results from Eq. (13), in this régime vortex motion in ideal, i.e. pinning-free, superconducting films is controlled by viscous forces only and consequently all information about a possible melting transition of the vortex lattice is lost in this case. As it will be shown in the subsequent discussion, vortex pinning, unavoidable in real films, provides the essential mechanism allowing the detection of melting phenomena of the vortex lattice.

B. Solid Vortex Phase With Pinning

If one assumes that vortex pinning does not seriously affect the dynamic response of the dislocations described by the dielectric constant (10), the equation of motion for the vortex continuum

is simply Eq. (8) with an additional force $-\nabla U(\vec{r})$ arising from the interaction of the vortices with a random pinning potential $U(\vec{r})$. It is well-known that Al-films prepared, as in our experiment, by evaporating the metal in a controlled oxygen atmosphere consist of a random distribution of metallic grains. The resulting structural inhomogeneities act to pin vortices by interaction with their normal cores. Since the grain size is usually much less than the core diameter, which is of the order of the coherence length, the pinning potential $U(\vec{r})$ is weak and can be treated as a perturbation [14]. In the experiments described in Section II, however, we found evidence also for strong pinning effects, possibly associated with a dilute random distribution of holes, which are known to be very efficient pinning centers [10]. We think, therefore, that in our films $U(\vec{r})$ will behave in a way somewhat similar to that sketched in Fig. 6, where a dilute random distribution of deep potential wells (holes) is superposed to the weak small-scale random potential due to the grains. In order to perform an explicit calculation of Z_v, the strong pinning component of $U(\vec{r})$ is approximated by a random distribution of deep parabolic wells of equal strength and, on the average, a distance L apart. In the dilute limit considered here we assume $L >> a$. The weak pinning part of $U(\vec{r})$ is represented by randomly distributed shallow parabolic wells. In the equilibrium configuration each well is occupied by a vortex sitting at the bottom of the well. Using this model, a calculation within the framework of the so-called Coherent Potential Approximation (CPA) shows [15] that Z_v is still given by Eq. (13) where, however, the relaxation rate τ_q^{-1} is replaced by :

$$\tau^{-1} = \tau_q^{-1} + \tau_L^{-1} + \tau_o^{-1} \qquad (15)$$

In this expression τ_L^{-1} is the relaxation rate of lattice modes with a wavelength of the order of ~ L which are induced by the strong component of $U(\vec{r})$:

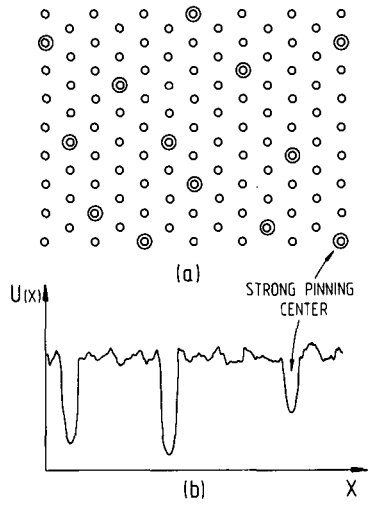

Fig. 6 : (a) Vortex lattice with randomly distributed strong pinning centers (holes).

(b) Profile of the random pinning potential U(x) along a selected direction x. The weak random potential between the strong wells (holes) represents vortex pinning arising from the granular nature of the Al-films.

$$\tau_L^{-1} \approx \frac{\mu}{\eta\varepsilon(\omega)} \frac{1}{L^2} \,. \tag{16}$$

τ_0, on the other hand, is the relaxation time of a single vortex in a shallow parabolic well and, therefore, does not depend on $\mu_R = \mu/\varepsilon(\omega)$.

Eq. (15) has a simple physical interpretation. For long-wavelength Fourier components of the driving force, such that $qL << 1$, the presence of strong pinning centers at an average distance L from each other causes the excitation of lattice deformations of much shorter wavelengths, of the order

of ~ L. For this case, the response of the vortex medium is strongly influenced by pinning, and the lattice relaxation rate is much faster than in a pinning-free situation ($\tau_L^{-1} >> \tau_q^{-1}$). In the opposite limit (qL >> 1) the strong pinning centers have little effect on the lattice response.

Typically, for our Al-films we expect a << L << R_i. Then, since $\tau_q^{-1} << \tau_L^{-1}$ for the relevant modes of the Corbino-disk geometry, from Eq. (13) one obtains :

$$Z_v = R_f\left[1 + \frac{i}{\omega\tau}\right]^{-1} , \qquad (17)$$

where $R_f = (R_{f\square}/2\pi)\ln(R_o/R_i)$ is the flux-flow resistance of the Corbino disk and $\tau^{-1} \simeq \tau_L^{-1} + \tau_o^{-1}$ in this case. In the low-temperature solid vortex phase ($T << T_M$), where only a few bound pairs of dislocations are thermally excited ($\varepsilon \simeq 1$), estimates of τ_L using reasonable values of L (L ≃ 10 - 50 μm) and of τ_o [2] show that $\omega\tau << 1$ at our frequencies. Then, from Eq. (17) it follows that $Re[Z_v] = R_f(\omega\tau)^2$ and $Im[Z_v] = R_f(\omega\tau)$ and, consequently, $Re[Z_v] << Im[Z_v]$, a result which clearly shows the importance of pinning in reducing the dissipation and in enhancing the inductive response of the solid vortex phase. As discussed in Section II, this prediction of the model agrees with our low-temperature experimental data (Figs. 2 and 3). Under certain conditions, both $Re[Z_v]$ and $Im[Z_v]$ exhibit, for $T \gtrsim T_M$, frequency-dependent structures, which reflect the peculiar behaviour of $\varepsilon^{-1}(\omega)$ in this intermediate temperature region (see Section III A). These features will be discussed in more detail later on in this paper (Section III D). In the high temperature fluid vortex phase ($T >> T_M$) the presence of a large number of free dislocations leads to a vanishingly small $\varepsilon^{-1}(\omega)$ and thus $\tau \simeq \tau_o$. In this case, Z_v reduces to the expression for a single vortex, as one actually expects for a liquid in which particles are uncorrelated. However, our model is a typical "solid" model in which the displacement field $\vec{u}$

describes deformations with respect to a fixed equilibrium structure. Thus, Z_v, which is proportional to the vortex mobility, vanishes in the limit $\omega = 0$. Since this is clearly not the case for a liquid, where the dc mobility is finite, in the next subsection we discuss the response of the fluid vortex phase in presence of thermal fluctuations.

C. Fluid Vortex Phase With Pinning

Since the potential wells associated with the strong pinning centers are assumed to be very deep (with activation energy much larger than k_BT) and dilute ($L >> a$), the contribution of vortices sitting in these wells to the overall vortex impedance of the fluid phase well above T_M is expected to be very small. For this reason we consider a model in which all vortices interact only with the weak component of the pinning potential, namely that associated with the granular structure of the Al-films. For $T >> T_M$ vortex motion is uncorrelated, so that it is sufficient to consider the Brownian motion of an individual vortex in the random pinning force field. To our knowledge, the problem of finding the frequency-dependent mobility of such a particle has not been studied in detail. However, a solution containing all the essential physical features can be easily obtained from a 1D model in which the random potential $U(\vec{r})$ is replaced by a 1D sinusoidal field $U(x) = U \cos qx$. In this case, the Langevin equation of motion for a vortex of mass m can be written as :

$$m\ddot{x} = - \eta'\dot{x} + U_0 q \sin qx + f(t), \tag{18}$$

where $\eta' = \eta/n_\square$ ($n_\square = B/\phi_0$ is the areal vortex density) and $f(t)$ is the fluctuating Langevin force with a white-noise spectrum defined by the correlation function

$$\langle f(t)f(t')\rangle = 2\eta' k_BT \delta(t - t') . \tag{19}$$

The frequency-dependent vortex mobility, which is the Fourier transform of the velocity-velocity correlation function, and, consequently, Z_v can now be deduced from Eq. (18) using the continued-fraction method first applied by Fulde et al. [16] to a similar problem. In the so-called Smoluchowski limit, where the viscous force dominates over the inertial force in Eq. (18), a two-pole continued fraction expansion leads to :

$$Z_v = R_f\left[1 + \frac{\tau_D/\tau_o'}{1 - i\omega\tau_D}\right]^{-1} , \qquad (20)$$

where $\tau_D^{-1} = D_v q^2$ is the vortex diffusion rate over distances of the order of the wavelength of the periodic pinning potential ($D_v = k_B T/\eta'$ is the vortex diffusion constant). The relaxation time ratio τ_D/τ_o' is given by :

$$\frac{\tau_D}{\tau_o'} = [I_o^2(y) - 1] , \qquad (21)$$

where $y = U_o/k_B T$ and τ_o' is related to τ_o [Eq. (15)] by $\tau_o' = \tau_o\ I_o(y)/I_1(y)$. $I_o(y)$ and $I_1(y)$ are modified Bessel functions. In the low-frequency limit ($\omega\tau_D << 1$) from Eq. (20) one deduces :

$$Re[Z_v] = \frac{R_f}{I_o^2(y)} , \quad Im[Z_v] = R_f\ \omega\tau_D\ \frac{I_o^2(y) - 1}{I_o^4(y)} . \qquad (22)$$

These expressions show that, at low frequencies, the dissipative component of Z_v is independent of ω, whereas the dispersive component scales linearly with ω. Moreover, as one easily deduces from the properties of $I_o(y)$, both $Re[Z_v]$ and $Im[Z_v]$ exhibit a thermally activated behaviour and $Re[Z_v] > Im[Z_v]$. These are precisely the features shown by our high-temperature experimental results (Fig. 2 and 3), which can indeed be fitted to the above theoretical expressions. Assuming that, near T_c, $R_f \simeq R_{n\square}B/H_{c2}(T) \sim [1 - (T/T_c)]^{-1}$ and that U_o varies with temperature as the superfluid density, i.e. $U_o(T) = U_{oo}[1 - (T/T_c)]$ near T_c, one obtains an acceptable fit of the data for Al

using $U_{oo} \approx 50$ K and $\tau_D \approx 2 \times 10^{-5}$ s. This value of U_{oo} is consistent with an estimate of Fisher [2] for granular films, who finds $U_o(T_M)$ of the order of $k_B T_M$ in films whose T_M is relatively close to T_c. Moreover, using the Bardeen-Stephen theory [9] to calculate η', from τ_D we infer $\lambda_p = 2\pi/q \sim 35$ μm. Because of the random nature of the pinning potential operating in our films, it is difficult to assess the significance of this figure.

D. The Transition Region

A description of the pinned vortex medium at intermediate temperatures ($T \gtrsim T_M$) is difficult and certainly requires a more detailed theoretical treatment. From a phenomenological point of view, however, it is possible to describe its dynamic response in the vicinity of the melting transition using a simple interpolation scheme. With this in mind we write for the vortex impedance Z_v :

$$Z_v = R_f \left[1 + \frac{\tau_D^*/\tau}{1 - i\omega\tau_D^*} \right]^{-1} , \qquad (23)$$

where τ is still given by $\tau^{-1} \approx \tau_L^{-1} + \tau_o^{-1}$. Well above T_M ($T >> T_M$), in the fluid vortex phase, $\varepsilon^{-1}(\omega)$ vanishes and, consequently, $\tau \approx \tau_o$. If τ_D^* is identified as the vortex diffusion time τ_D defined in *III C.*, then Eq. (23) becomes identical to Eq. (21), the dynamic response of the vortex fluid. On the other hand, if τ_D^* becomes very large ($\tau_D^* \to \infty$), Eq. (23) transforms into the vortex impedance of the pinned solid vortex phase Eq. (17) . These considerations show that the dynamic response of the vortex medium in the transition region ($T \gtrsim T_M$) can be described in simple terms if one assumes that in Eq. (23) τ_D^* diverges as one approaches the melting temperature T_M from above, i.e. $\tau_D^* \to \infty$ as $T \approx T_M^+$. It seems therefore natural to identify τ_D^*, for $T \gtrsim T_M$, as the time free dislocations need to diffuse over distances of the order of the correlation length $\xi_+(T)$ [see

Eq. (12)] in the fluid vortex phase, i.e. $\tau_D^* \simeq \xi_+^2(T)/D$. Relying on this phenomenological approach, we have determined the vortex impedance near the solid-liquid phase transition from Eq. (23) using Eq. (10) for $\varepsilon(\omega)$. To this purpose the contribution $\varepsilon_b(\omega)$ associated with thermally excited bound pairs of dislocations has been calculated using the procedure described in Ref. [13]. Three parameters enter this calculation, namely $\ell \simeq \ell n[(D/\omega)^{1/2}/a]$, $\mu/\mu_R(T_M^-)$ and s. Since estimates of D are not available so far, we have set $D \simeq D_v$ obtaining $\ell \sim 7$ for a frequency of 1 kHz and $a \simeq 1$ μm, which correspond to B ≃ 20 gauss. To be consistent with Fisher's estimate [2], we have chosen $\mu/\mu_R(T_M^-) = 2$. Then, setting $s = 2\pi$, $\omega\tau_o = 10^{-3}$ and $\omega\tau_L = 10^{-4}$ at low temperatures, where $\varepsilon \simeq 1$, we obtain the results shown in Fig. 7. A peak in dissipation and a shoulder in the inductive component of Z_v show up approximately at the temperature T_ω defined in Section III A [$\xi_+^2(T_\omega) \simeq D/\omega$]. These

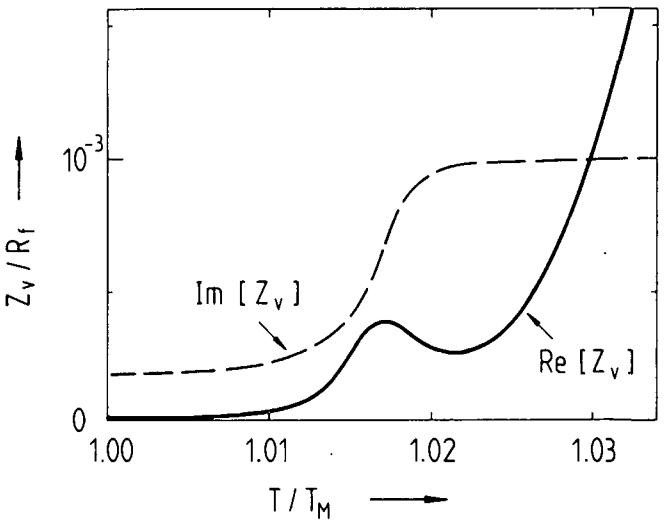

Fig. 7 : Real and imaginary part of the complex vortex impedance as a function of temperature in the vicinity of the melting transitions as deduced from Eq. (23).

structures are a manifestation of the unique behaviour of $\varepsilon^{-1}(\omega)$ in the vicinity of T_M. If one lowers the frequency, while keeping all other parameters fixed, the characteristic structures of Fig. 7 are still well resolved but their intensity decreases approximately linearly with ω. At higher frequencies, the structures at T_ω are washed out. Notice that the results shown in Fig. 7 confirm the already discussed and experimentally observed crossover from $\mathrm{Re}[Z_v] < \mathrm{Im}[Z_v]$ in the low-temperature solid vortex phase to $\mathrm{Re}[Z_v] > \mathrm{Im}[Z_v]$ in the high-temperature fluid vortex phase.

The model discussed above shows that vortex pinning plays an essential role in experiments probing characteristic features of dislocation-mediated melting. Whether the structures emerging in our experimental data just above the predicted melting temperature can be understood on the basis of the present model remains, however, an open question. It is possible that the small peak in the 990 Hz-data of A1*1* results from the dislocation unbinding mechanism. As predicted by the model, it disappears, in fact, at higher frequencies and is probably blurred by noise at lower frequencies. Further experimental work, however, is necessary in order to ascertain this conjecture. Unexplained by the present treatment are the well-resolved peak structures observed for A1*2*, which do not shift with ω, and whose intensity is by far too large to be accounted for by our model. As already mentioned in Section II, their explanation will probably require the development of a more elaborate non-linear theory.

As a final point, we would like to stress an intrinsic difficulty one faces in experiments probing melting phenomena of a lattice of superconducting vortices. Unlike the case of the superfluid transition in 2D superfluid He-films [13] and in 2D superconducting films [17], where it is possible to couple the driving field directly to the vortex excitations, in experiments probing the shear modulus of a lattice of vortices the external

force couples primarily to the total displacement field of an elastic continuum with thermally excited dislocations and not directly to the dislocation field. As a consequence, characteristic features arising from the dislocation-unbinding transition are difficult to observe. In this paper we have shown that vortex pinning is an essential tool to overcome this difficulty. We think that experiments dealing with well-controlled pinning structures [10,18] will prove to be very useful in ascertaining the nature of the melting transition.

ACKNOWLEDGMENTS - One of us (P.M.) is very grateful to A.F. Hebard for valuable discussions concerning possible experiments, in particular the Corbino-disk experiment, on vortex-lattice melting. Moreover, we gratefully acknowledge the help of M. Puga and Ph. Renaud in the theoretical development. This work has been supported by the Swiss National Science Foundation.

REFERENCES

[1] B.A. HUBERMAN and S. DONIACH, Phys. Rev. Lett. 43, 950 (1979).

[2] D.S. FISHER, Phys. Rev. B 22, 1190 (1980).

[3] J.M. KOSTERLITZ and D.J. THOULESS, J. Phys. C 6, 1181 (1973).

[4] A.T. FIORY and A.F. HEBARD, Phys. Rev. B 25, 2073 (1982).

[5] D.R. NELSON and B.I. HALPERIN, Phys. Rev. B 19, 2457 (1979).

[6] A. ZIPPELIUS, B.I. HALPERIN and D.R. NELSON, Phys. Rev. B 22, 2514 (1980).

[7] M.P. SHAW and P.R. SOLOMON, Phys. Rev. 164, 535 (1967).

[8] A.F. HEBARD and A.T. FIORY, Physica 109 & 110B, 1637 (1982).

[9] J. BARDEEN and M.J. STEPHEN, Phys. Rev. 140, A1197 (1965).

[10] A.T. FIORY, A.F. HEBARD and S. SOMEKH, Appl. Phys. Lett. 32, 73 (1978).

[11] V. AMBEGAOKAR, B.I. HALPERIN, D.R. NELSON and E.D. SIGGIA, Phys. Rev. B 21, 1806 (1980).

[12] A.M. KOSEVICH, in Dislocations in Solids, Edited by F.R.N. NABARRO (North-Holland, 1979) p. 33.

[13] D.J. BISHOP and J.D. REPPY, Phys. Rev. B 22, 5171 (1980).

[14] A. SCHMID and W. HAUGER, J. Low Temp. Phys. 11, 667 (1973).

[15] H. BECK and P. RENAUD, to be published.

[16] P. FULDE, L. PIETRONERO, W.R. SCHNEIDER and S. STRÄSSLER, Phys. Rev. Lett. 35, 1776 (1975).

[17] A.F. HEBARD and A.T. FIORY, Phys. Rev. Lett. 44, 291 (1980).

[18] O. DALDINI, P. MARTINOLI, J.L. OLSEN and G. BERNER, Phys. Rev. Lett. 32, 218 (1974).

Physica 107B (1981) 455-458
North-Holland Publishing Company

LOCKING-UNLOCKING TRANSITION OF A TWO-DIMENSIONAL LATTICE OF SUPERCONDUCTING VORTICES

P. Martinoli, H. Beck, M. Nsabimana and G.-A. Racine

Institut de Physique, Université de Neuchâtel,
CH-2000 Neuchâtel, Switzerland

At a temperature $T_u < T_c$ a two-dimensional lattice of superconducting vortices interacting with a periodic pinning potential is found to undergo a transition from a registred locked phase ($T < T_u$) to a floating unlocked phase ($T > T_u$). A simple model accounts for the main features of the transition observed in thickness-modulated superconducting films.

Two-dimensional (2D) systems have received considerable attention recently. In several experiments the 2D crystal under consideration interacts with the force field created by a periodic substrate. Among other situations, this is the case of the 2D vortex lattice in thin superconducting films, whose thickness is periodically modulated in one direction [1]. In this letter we report on a novel phase transition we have observed in this particular physical system. As the temperature T is raised above a certain critical value T_u, a lattice of vortices in registry with the periodic film structure undergoes a transition from a locked (or pinned) L-phase to an unlocked (or unpinned) U-phase. The U-phase is expected to be in the liquid state.

In previous experiments [1] we have shown that the critical currents $I_c(B)$ and the RF-properties of thickness-modulated superconducting layers in the flux-flow régime are very sensitive to the 1D periodic potential associated with the particular film profile. Peak structures appear in the $I_c(B)$-curves whenever the vortex lattice matches the periodic substrate, a situation occuring if $\vec{q} = \vec{g}$, $\vec{q}$ being the wave vector of the modulation and $\vec{g}$ a reciprocal vortex lattice vector. An additional signature of the periodic film structure is the presence of steps in the I-V characteristics of modulated films exposed to RF-radiation. Pinning induced coupling at RF-frequencies between the oscillating motion of the vortex lattice in a registred configuration and the electromagnetic field results in quantum interference transitions at discrete values $E_n = nf\lambda_g B$ of the flux-flow dc-electric field (f is the frequency of the RF-radiation, $\lambda_g = 2\pi/q$ the wave-length of the modulation and n an integer).

The experiments reported here were performed on granular Al-films with sheet resistances, $R_\square = \rho/d$, ranging typically from 10 to 100 Ω. A combined holographic-photolithographic technique was used to obtain grating-like film profiles with $\lambda_g \lesssim 1$ μm. To meet the condition for the weak pinning limit discussed below, the relative thickness modulation never exceeded ~ 10%. Peak structures in the $I_c(B)$-curves of an Al-film with $R_\square = 35$ Ω are shown in Fig. 1

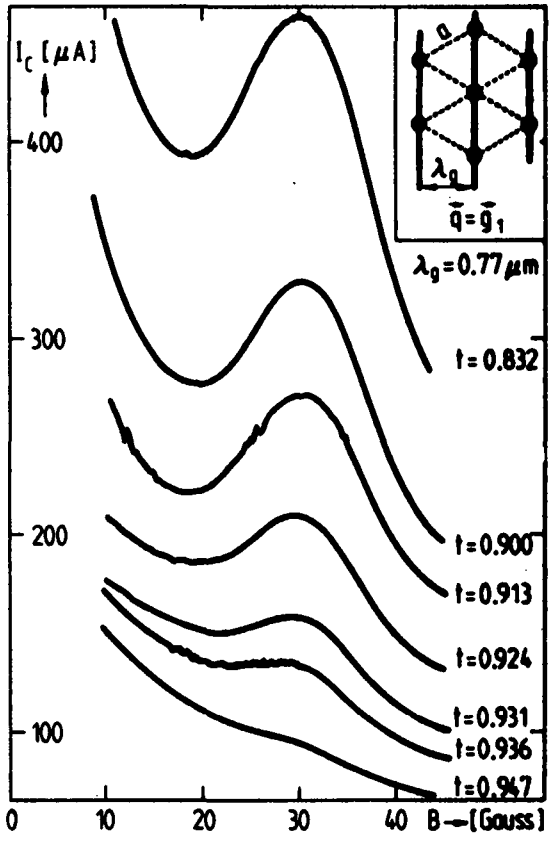

Fig. 1 : Magnetic field dependence of the critical currents of a thickness-modulated Al-film ($R_\square = 35$ Ω, $T_c = 2.16$ K, $t = T/T_c$).

for the fundamental matching configuration defined by $a = 2\lambda_g/\sqrt{3}$ (or, equivalently, $B = (\sqrt{3}/2)\varphi_o/\lambda_g^2$) and sketched in the insert. It is seen that, with rising temperature, a relatively rapid degradation of the I_c-maxima occurs as one approaches a critical temperature T_u of ~ 2.05 K. For $T > T_u$ the structures in $I_c(B)$ completely disappear indicating that the vortex lattice is no longer locked to the periodic substrate. I-V

0378-4363/81/0000–0000/$02.50

characteristics and their derivatives for an Al-film ($R_\square$ = 15 Ω) exposed to 100 MHz-radiation of constant power are shown in Fig. 2. As in the critical current case, from the evolution of the n = 1-interference transition with increasing temperature one is led to the conclusion that

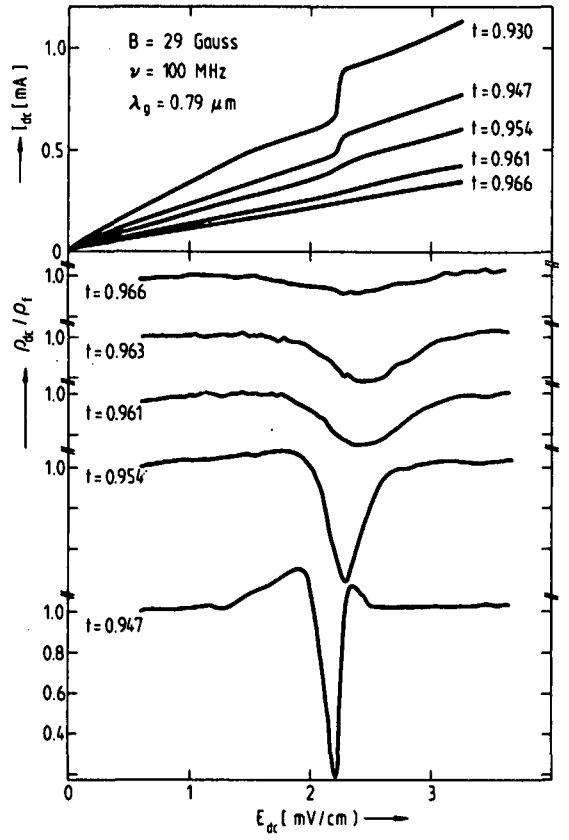

Fig. 2 : RF-excited current-voltage characteristics and their derivatives for a thickness-modulated Al-film ($R_\square$ = 15 Ω, T_c = 1.90 K, t = T/T_c).

dynamic coupling of the matched vortex lattice to the periodic potential is totally absent for $T > T_u \approx 1.84$ K. Notice that the n = 1-step is correctly located at $E_1 = f\lambda_g B$ for $T \ll T_u$ but that it gradually shifts to higher voltages in the immediate vicinity of T_u. This effect might be due to an enhanced thermal expansion of the vortex lattice near T_u, but is still not fully understood at present. For both the static and dynamic interactions described above, T_u is found to scale linearly with increasing $R_\square$.

A simple model accounts for the main features observed in our experiments. At finite temperatures the vortices execute, for $\vec{q} = \vec{g}$, a brownian motion around the equilibrium position they would assume at the bottom of the potential wells at T = 0. Accordingly, the equation of motion for a vortex at the lattice site $\underline{\ell}$ can be written as :

$$\eta \dot{\vec{u}}_{\underline{\ell}} = -\sum_{\underline{\ell}'} \tilde{G}(\underline{\ell}-\underline{\ell}')\vec{u}_{\underline{\ell}'} - \vec{q}\Delta'\sin(\vec{q}\cdot\vec{u}_{\underline{\ell}}) + \vec{F}_{\underline{\ell}}(t) \qquad (1)$$

where the four terms represent, successively, the viscous damping force, the lattice restoring force, the pinning force and the fluctuating Langevin force acting on the vortex $\underline{\ell}$. η is the viscosity coefficient, $\tilde{G}(\underline{\ell}-\underline{\ell}')$ the elastic matrix and 2Δ' the height of the potential barrier. $\vec{F}_{\underline{\ell}}(t)$ is defined by the correlation function

$$\langle F^{\alpha}_{\underline{\ell}}(t) F^{\beta}_{\underline{\ell}'}(t')\rangle = (2\eta k_B T/d)\,\delta_{\alpha\beta}\delta_{\underline{\ell}\underline{\ell}'}\delta(t-t').$$

Within the framework of the so-called renormalized harmonic approximation, Eq. (1) can be solved for the mean square fluctuation $\langle u^2\rangle$ of the vortices using a Fourier transform technique. Since only transverse (t) modes are relevant in a vortex lattice, one obtains in the weak pinning limit ($\Delta \ll \mu$) :

$$\langle u_t^2\rangle = (k_B T/4\pi\mu)\,\ell n\,(\mu/\Delta_R) \qquad (2)$$

where μ is the shear modulus and Δ_R an effective strength of the pinning potential given by

$$\Delta_R = \Delta \exp(-q\langle u_{tx}^2\rangle/2) \qquad (3)$$

where $\Delta = d(B/\varphi_0)\Delta'$. Eq. (3) shows how the renormalization enters our problem : through a Debye-Waller factor associated with the components u_{tx} of the transverse thermal fluctuations along the direction x ($// \vec{q}$) of the thickness modulation. Since, by equipartition, $\langle u_{tx}^2\rangle \approx (\frac{1}{2})\langle u_t^2\rangle$ in the limit $\Delta \ll \mu$, from Eqs. (2) and (3) one deduces :

$$\Delta_R/\Delta = (\Delta/\mu)^{t_u/(1-t_u)} \qquad (4)$$

where $t_u = T/T_u$. T_u is given by

$$k_B T_u = (4/\pi)\mu(T_u)\lambda_g^2 \qquad (5)$$

an expression also derived by Pokrovsky and Talapov [2] using a different method.

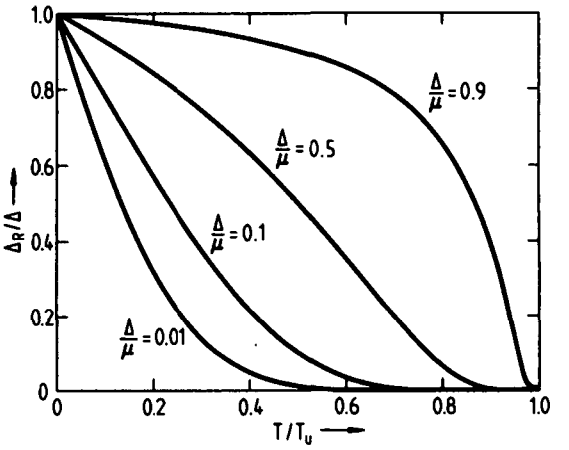

Fig. 3 : Temperature dependence of the effective pinning barrier [Eq. (4)].

From Fig. 3, where Δ_R/Δ is plotted as a function of t_u, it clearly results that at T_u the vortex lattice undergoes a transition from a registred L-phase ($\Delta_R \neq 0$) to a "floating" U-phase ($\Delta_R = 0$). Unlike a 2D lattice on a flat substrate, $\langle u^2 \rangle$, as shown by Eq. (2), is finite in the L-phase. Moreover, since the melting temperature [3] for a pinning free vortex lattice is lower than T_u, the U-phase is expected to be in the liquid state. It is argued, therefore, that our experiments reflect a direct transition from a solid registred L-phase to a fluid-like U-phase [4].

We conclude by observing that T_u is always lower than T_c, the BCS transition temperature. For T_u close to T_c, Eq. (5) can be written in the form $T_u/T_c \approx 1 - 0.31\ (R_\square/R_u)$ where $R_u = \hbar/e^2 = 4.11$ kΩ. This qualitatively agrees with the experimentally observed linear dependence of T_u on $R_\square$.

We thank J.R. Clem for fruitful discussions in the early stage of these investigations. This work was supported by the Swiss National Science Foundation.

REFERENCES :

[1] Martinoli, P. and Clem, J.R., AIP Conf. Proc. 58 (1980) 176-185 and references quoted therein.

[2] Pokrovsky, V.L. and Talapov, A.L., Phys. Rev. Lett. 42 (1979) 65-67.

[3] Doniach, S. and Huberman, B.A., Phys. Rev. Lett. 43 (1979) 950-952.

[4] Nelson, D.R. and Halperin, B.I., Phys. Rev. B19 (1979) 2457-2484.

Helvetica Physica Acta, Vol. 55 (1982) 655–668 0018–0238/82/060655–14$1.50 + 0.20/0

Locked and unlocked phases of a two-dimensional lattice of superconducting vortices

By P. Martinoli, M. Nsabimana, G. A. Racine and H. Beck,
Institut de Physique, Université de Neuchâtel,
CH–2000 Neuchâtel, Switzerland
J. R. Clem, Ames Laboratory–USDOE and Department of Physics, Iowa State University, Ames, Iowa 50011, USA

(23. XI. 1982)

Abstract. The flux lattice in a thin film of a type II superconductor, whose thickness is periodically modulated, allows for an investigation of various phase transitions typical of two-dimensional systems. We present a continuum approach in which the mismatch δ between the equilibrium lattice structure and the spacial period of the modulation plays a major role. In the ground state the lattice is locked by the modulation potential when δ is small, whereas for large enough δ the lattice is freely floating, its structure showing periodic discommensurations. A phase diagram in the (δ, T)-plane can be established by taking into account thermal fluctuations. Critical current data at various temperatures show good agreement with the theoretical predictions.

I. Introduction

Phase transitions in two-dimensional (2D) systems have received considerable attention recently. In several experiments the 2D crystal under consideration is exposed to the force field created by a periodic substrate. Among other situations, this is the case of a 2D lattice of superconducting vortices interacting with a periodic pinning potential. As pointed out by Martinoli and coworkers [1] some years ago, thin superconducting films, whose thickness is periodically modulated in one direction, provide such a system. In this paper we show how critical current measurements in thickness modulated layers can be used to probe a locking–unlocking phase transition of the 2D vortex lattice occurring when the conditions of flux line density and/or temperature are changed in this particular physical system. Some aspects of the locking–unlocking transition were reported in a recent letter [2]. Here we describe it in more detail.

The phase diagram of 2D crystals in a periodic potential has been studied by a number of authors [3]. Dealing with situations where the periodic substrate is, as in our case, anisotropic, a recent theory by Pokrovsky and Talapov [4] (PT) is particularly relevant to the understanding of our experiments, where the 2D vortex lattice experiences the 1D periodic force field created by the thickness modulation. At absolute zero ($T = 0$), PT predict the existence of stable locked (L)-phases when the degree of mismatch between the natural (undistorted) lattice and the underlying periodic pinning structure does not exceed some critical value.

In an L-phase the vortex lattice is a 2D epitaxial (or commensurate) solid in registry with the substrate periodicity. At the critical mismatch PT predict a second order transition from a registered L-phase to an incommensurate unlocked (U)-phase. In the U-phase the vortex lattice is a "floating" 2D solid characterized by the presence of a superstructure consisting in a 1D periodic sequence of domain wall dislocations. These and other interesting features of the LU-phase transition at $T=0$ are discussed in Section II.A.

At finite temperatures thermal fluctuations of the vortices in the L-phase tend to unlock the vortex lattice from the periodic pinning structure, thereby driving the transition to the U-phase at a sufficiently high temperature. As a consequence of Brownian motion of the vortices, the critical degree of mismatch tolerated by an L-phase becomes smaller and smaller as the temperature rises and finally vanishes at a critical temperature T_{LU}, above which an L-phase can no longer exist. The corresponding LU-phase boundary has been calculated by PT using a renormalization-group technique [4]. In Section II.B we propose an alternative approach based on the more transparent Self-Consistent Harmonic Approximation (SCHA). The expression for T_{LU} deduced from this model agrees with that obtained by PT but the shape of our LU-phase boundary differs considerably from that of PT. For instance, our phase diagram does not show the rather surprising reentrant behaviour which one deduces by inspection of the PT-theory. It is further argued that, above T_{LU}, the vortex lattice is a 2D floating solid exhibiting topological order [5] or a liquid according to whether T_{LU} is lower or higher than T_M, the temperature at which the vortex lattice is expected to melt through thermal dissociation of bound pairs of dislocations [5–7].

Pinning phenomena in thickness modulated superconducting films prove to be a sensitive probe of the LU-phase transition. Since in an L-phase the vortex lattice is obviously pinned by the periodic film structure while in a U-phase it is free to slide under the influence of an arbitrarily small driving force, characteristic peaks reflecting the presence of various L-phases show up in the critical current curves $I_c(B)$ [1]. As the magnetic field B governs the vortex density, the width of the peaks is a measure of the critical mismatch at which the LU-phase transition takes place. With rising temperature the intensity of the I_c-maxima decreases and finally undergoes a relatively rapid degradation as one approaches a critical temperature which we identify with T_{LU}. For $T > T_{LU}$ the structures in $I_c(B)$ are completely washed out indicating that the vortex lattice is no longer locked to the periodic substrate. These and other features of our I_c-data are discussed in Section III in the light of the theoretical predictions of the previous section.

II. Theoretical considerations

(A) *Phase transition at zero temperature*

Let us first briefly recall some of the basic concepts and results of the PT-theory [4]. To this purpose we consider a 2D triangular lattice of superconducting vortices, with lattice parameter a, in static interaction with a 1D harmonic potential of amplitude Δ and wave vector $\vec{q}$ ($q = 2\pi/\lambda_g$). We shall focus our attention on situations where $\vec{q}$ is very close to one of the vectors, $\vec{g}$, of the reciprocal vortex lattice, the condition $\vec{q} = \vec{g}$ defining a configuration of perfect

matching between the (undistorted) lattice and the sinusoidal pinning potential. It is assumed that the lattice of Abrikosov vortices is incompressible [8] and, further, that the pinning is weak when compared to the lattice stiffness, i.e. $\Delta < \mu$, where μ is the shear modulus of the vortex lattice [9]. Under these conditions only long wavelength shear deformations turn out to be relevant and, as a consequence, the vortex lattice can be treated as an elastic continuum. Then, the energy of the system can be written as the sum of an elastic contribution and of the potential energy due to the periodic pinning force

$$\mathscr{E} = \int \left[\frac{\mu}{2} \left(\frac{\partial u}{\partial y} + \frac{\partial v}{\partial x} \right)^2 + \Delta(1 - \cos q\phi) \right] dx\, dy. \tag{1}$$

In writing this expression we have jumped ahead to the conclusion of PT asserting that the lowest energy configuration of the vortex lattice is characterized by a quasi 1D deformation field $\vec{w}$ which, in an $x' - y'$ reference frame with x' pointing in the $\vec{q}$-direction, has components of the form

$$u' = -\delta x' + \phi(x), \qquad v' = \delta y' - \phi(x), \tag{2}$$

where $\delta = 1 - (g/q)$ measures the degree of mismatch. These expressions clearly show that there are two distinct contributions to $\vec{w}$. The first one is an area conserving deformation resulting from a uniform compression ($\delta > 0$) or expansion ($\delta > 0$) $-\delta x'$ along x' combined with a uniform expansion ($\delta > 0$) or compression ($\delta < 0$) $\delta y'$ along y'. This deformation is chosen such that the potential energy contribution to $\mathscr{E}$ vanishes: the vortices are forced to lie in the valleys of the cosine-potential. Superposed to this uniform field is a 1D deformation $\phi(x)$ which, for an incompressible lattice, is found to propagate in a direction x forming an angle of 45° with $\vec{q}$ [4, 8]. Thus, in the x-y coordinate system rotated by 45° with respect to $x' - y'$ the deformation field $\vec{w}$ has the components

$$u = \delta y, \qquad v = \delta x - \sqrt{2}\, \phi(x). \tag{3}$$

As it clearly emerges from these expressions, in the new reference system the uniform deformation described in connection with equation (2) results from the superposition of two uniform shear deformations, one along x and the other along y. By inserting u and v, as given by equation (3), into the general form of the elastic energy of an isotropic 2D continuum [4] one immediately obtains equation (1).

To determine $\phi(x)$, we simply minimize the functional $\mathscr{E}[\phi(x)]$ with respect to $\phi(x)$, thereby obtaining the following sine–Gordon equation [10] for the "phase" field $\Phi(x) = q\phi(x)$

$$\sin \Phi - l^2 \frac{\partial^2 \Phi}{\partial x^2} = 0, \tag{4}$$

where $l^2 = 2\mu/\Delta q^2$. Its solution in terms of elliptic functions

$$\Phi(x) = \pi + 2am(x/kl) \tag{5}$$

is a stair-shaped function representing a regular sequence of kinks (discommensurations), whose period L is related to k by

$$L = 2klK(k), \tag{6}$$

where $K(k)$ is a complete elliptic integral of the first kind. Using equations (5) and (6), the potential energy (1) can be expressed as a function of the variational parameter k. Minimization of $\mathscr{E}(k)$ with respect to k leads to the condition

$$\delta = \frac{2}{\pi}\left(\frac{\Delta}{\mu}\right)^{1/2}\frac{E(k)}{k}, \tag{7}$$

where $E(k)$ is a complete elliptic integral of the second kind. From the properties of $E(k)$ it follows that there are solutions of equation (7) satisfying the condition $0 \leqslant k \leqslant 1$ only if δ is larger than a critical mismatch δ_c given by

$$\delta_c = \frac{2}{\pi}\left(\frac{\Delta}{\mu}\right)^{1/2}. \tag{8}$$

For $|\delta| \geqslant \delta_c$ $\Phi(x)$ is of the form (5) and, as a consequence, the vortex lattice is in the incommensurate U-phase. This is shown in Fig. 1, where we have assumed that the starting matching configuration is that corresponding to $\vec{q} = \vec{g}_1$, $\vec{g}_1$ being one of the six nearest-neighbour reciprocal lattice vectors ($g_1 = 4\pi/a\sqrt{3}$). Since $\delta > 0$ for the configuration shown in Fig. 1, large portions of the lattice appear to be uniformly compressed along x' and expanded along y' and are essentially

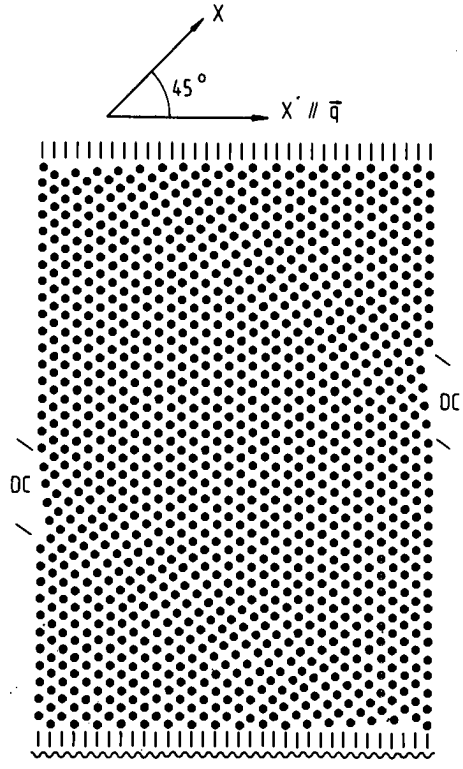

Figure 1
Incommensurate U-phase for $\delta = 0.13$ ($B/B_{10} = 0.76$). Discommensurations (DC) form a periodic 1D sequence propagating at 45° with respect to $\vec{q}$.

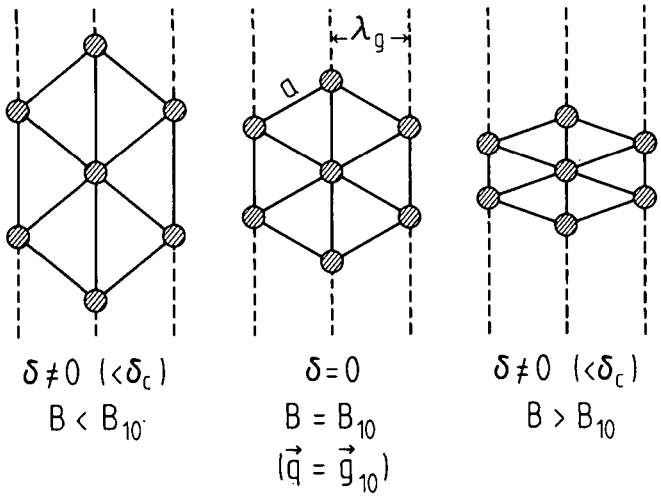

Figure 2
Three different deformation states of the fundamental commensurate L_{10}-phase.

commensurate to the underlying 1D periodic pinning structure. These regions are separated from each other by a 1D periodic sequence of domain wall discommensurations propagating at 45° with respect to $\vec{q}$. At the discommensuration sites the phase field $\Phi(x)$, which is essentially constant in the nearly commensurate regions between successive kinks, changes by 2π over distances of the order of $\sim kl$. The period L of the superstructure diverges logarithmically (see equation 6) as δ approaches δ_c ($k \to 1$).

For $|\delta| < \delta_c$ there are no solutions of equation (7) and, consequently, $\Phi(x)$ is no longer given by equation (5). In this case $\mathscr{E}$ has its minimum value when the potential energy term associated with the 1D pinning field on the right-hand side of equation (1) vanishes, i.e. when $\Phi(x) = 0$ everywhere. Obviously, this corresponds to the commensurate L-phase shown schematically in Fig. 2 for $\delta = 0$ (matching configuration $\vec{q} = \vec{g}_1$) and for vortex densities lower and higher than that corresponding to $\vec{q} = \vec{g}_1$.

The areal potential energy density, $F_\square$, of the vortex lattice can be written in the form

$$F_\square = 2\mu\delta^2 - 2\Delta\{[\delta/\delta_c E(k)]^2 - 1\}\theta(|\delta| - \delta_c), \tag{9}$$

where $\theta(z)$ is the Heaviside function: $\theta(z) = 1$ for $z > 0$, $\theta(z) = 0$ for $z < 0$. The first term on the right-hand side of Eq. (9) is the elastic energy density associated with the uniform deformations characterizing both the L- and the U-phase, whereas the second one arises from the phase field $\Phi(x)$ and, consequently, contributes to $F_\square$ only in the U-phase. $F_\square(\delta)$ is plotted in Fig. 3 together with the result of a calculation based on a discrete lattice model [8] where, however, only harmonic shear deformations of the vortex lattice were considered. With this important restriction the LU-phase transition occurs for $\delta = 0$, but other features turn out to be identical to those predicted by the PT-model. In particular, the U-phase is characterized by the presence of a sinusoidal transverse deformation of the lattice propagating in a direction at 45° with respect to $\vec{q}$. A more detailed

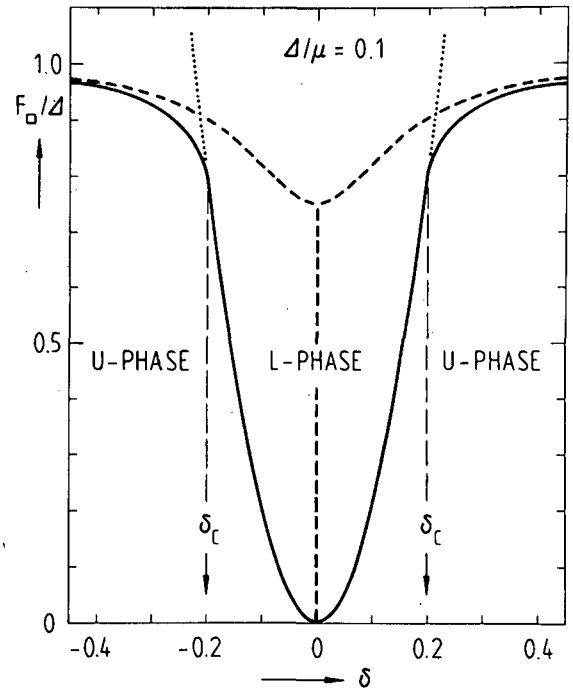

Figure 3
Areal energy density of a 2D lattice in a 1D periodic force field as a function of the mismatch δ. The full curve is based on equation (9). The dashed curve follows from a discrete lattice model allowing only for harmonic deformations. In this case the LU-transition occurs at $\delta = 0$.

account of the discrete lattice model, which proves to be very useful in the description of vortex lattice dynamics at high frequencies, will be published elsewhere.

(B) *Phase transition at finite temperatures*

To study the LU-phase transition at finite temperatures, we first consider the case of perfect matching ($\delta = 0$), which is particularly simple. For $\vec{q} = \vec{g}$ the vortices execute a Brownian motion around the equilibrium positions they would assume at the bottom of the potential wells at $T = 0$. Accordingly, the Langevin equation of motion for a vortex at the lattice site $\underline{l}$ can be written as

$$\eta \dot{\vec{u}}_{\underline{l}} = -\sum_{\underline{l}'}{}' \tilde{G}(\underline{l} - \underline{l}')\vec{u}_{\underline{l}'} - \vec{q}\Delta' \sin(\vec{q} \cdot \vec{u}_{\underline{l}}) + \vec{F}_{\underline{l}}(t), \tag{10}$$

where the four terms represent, successively, the viscous damping force, the lattice restoring force, the harmonic pinning force and the fluctuating Langevin force acting on the vortex at $\underline{l}$. $\eta^{-1} = R_{\square}/B\phi_0$, where $R_{\square}$ is the sheet flux-flow resistance of the superconducting film, is the mobility of a free vortex, $\tilde{G}(\underline{l} - \underline{l}')$ the elastic matrix and Δ' is related to Δ by $\Delta = (B/\phi_0)\Delta'$. $\vec{F}_{\underline{l}}(t)$ is assumed to have a

white noise spectrum defined by the correlation function

$$<F_{\underline{l}}^{\alpha}(t)F_{\underline{l}'}^{\beta}(t')=2\eta k_B T\delta_{\alpha\beta}\delta_{\underline{l}\underline{l}'}\delta(t-t') \tag{11}$$

stating that the Langevin force is uncorrelated in direction, space and time. To solve equation (10) for the mean square fluctuation $\langle u^2\rangle$ of the vortices it is convenient to expand $\vec{u}_{\underline{l}}(t)$ in normal modes of the vortex lattice

$$\vec{u}_{\underline{l}}(t)=\frac{1}{2\pi}\int_{-\infty}^{+\infty}\sum_{\underline{k},p}u_{\underline{k}}(\omega)\hat{e}_{\underline{k}p}e^{i(\vec{k}\cdot\vec{l}-\omega t)}\,d\omega, \tag{12}$$

where the $u_{\underline{k}}(\omega)$ are the normal mode amplitudes and the $\hat{e}_{\underline{k}p}$ are polarization vectors for longitudinal ($p=l$) and transverse ($p=t$) deformations. Linearizing the equation of motion (10) in the so-called Self-Consistent Harmonic Approximation (SCHA) and considering, as in Section II.A, only transverse modes of the vortex lattice, from equations (10) and (12) the following expression for the t-component, $u_{\underline{k}t}(\omega)$, of $\vec{u}_{\underline{k}}(\omega)$ is deduced

$$u_{\underline{k}t}(\omega)=\frac{F_{\underline{k}t}(\omega)}{D_{\underline{k}t}+\Delta_R(\vec{q}\cdot\hat{e}_{\underline{k}t})^2-i\eta\omega} \tag{13}$$

where $D_{\underline{k}t}$ is the matrix element of the (diagonal) dynamical matrix associated with transverse modes and $F_{\underline{k}t}(\omega)$ is the transverse Fourier component of the Langevin force. Within the framework of SCHA the effective strength, Δ_R, of the pinning potential experienced by the vortices is given by

$$\Delta_R=\Delta e^{-\frac{1}{2}q^2\langle u_{tx}^2\rangle} \tag{14}$$

where $\langle u_{tx}^2\rangle$ is the mean square transverse fluctuation along the direction x parallel to $\vec{q}$. Equation (14) shows very clearly how the renormalization effect of the thermal fluctuations, which is the essential feature leading to the LU-phase transition, enters our problem: through a Debye–Waller factor which reduces the amplitude of the periodic force field acting on the vortices. To calculate the mean square transverse fluctuation

$$\langle u_t^2\rangle=\frac{1}{\pi}\lim_{T\to\infty}\frac{1}{T}\int_0^{\infty}\sum_{\underline{k}}|u_{\underline{k}}(\omega)|^2\,d\omega, \tag{15}$$

we assume a Debye model, for which $D_{\underline{k}t}=\mu k^2$, and replace the sum over $\underline{k}$ in equation (15) by an integral over a smooth density of states. In the weak pinning limit $\Delta\ll\mu$ considered here we then deduce from equations (11), (13) and (15)

$$\langle u_t^2\rangle=\frac{k_BT}{4\pi\mu}\ln(\mu/\Delta_R). \tag{16}$$

This expression shows quite clearly that the L-phase, which for the case of perfect matching ($\delta=0$) under consideration is stable as long as Δ_R is finite, is a 2D solid with conventional long range order. As expected for 2D systems, $\langle u_t^2\rangle$ diverges logarithmically as Δ_R vanishes. Since, by equipartition, $\langle u_{tx}^2\rangle\approx\frac{1}{2}\langle u_t^2\rangle$ in the limit $\Delta\ll\mu$, from equations (14) and (16) one obtains

$$\Delta_R/\Delta=(\Delta/\mu)^{T/(T_{LU}-T)}, \tag{17}$$

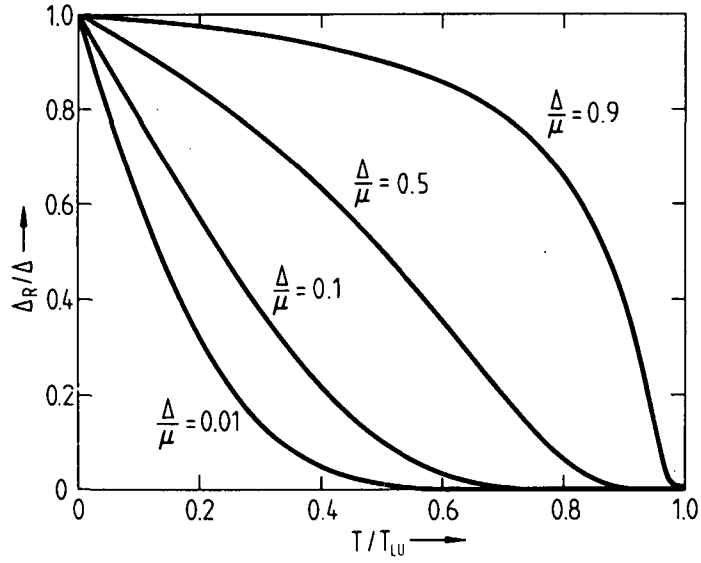

Figure 4
Temperature dependence of the effective pinning potential amplitude.

where T_{LU} is implicitly defined by

$$k_B T_{LU} = (4/\pi)\mu(T_{LU})\lambda_g^2. \tag{18}$$

From Fig. 4, where Δ_R/Δ is plotted as a function of T/T_{LU} for a set of (Δ/μ)-values, it clearly results that at T_{LU} the vortex lattice undergoes a transition from a perfectly matched L-phase ($\Delta_R \neq 0$) to a "floating" U-phase ($\Delta_R = 0$). It should be noticed that the expression (18) for T_{LU}, as deduced in our SCHA-scheme, is the same as that obtained with a renormalization-group technique by PT.

For a moderately dense lattice of vortices in dirty superconducting films μ can be written in the form [9]

$$\mu = \tfrac{1}{2} n_\square (\phi_0/4\pi)^2 \frac{1}{\Lambda}, \tag{19}$$

where $n_\square = B/\phi_0$ is the areal vortex density and $\Lambda = 2\lambda^2/d$ an effective penetration depth for 2D superconducting layers (d is the film thickness), whose temperature dependence is given by [11]

$$\Lambda^{-1}(T) = 2.17(4\pi/\phi_0)^2 (R_u/R_{n\square}) k_B T_c \left[\frac{\Delta(T)}{\Delta(0)} Tgh\left(\frac{\Delta(T)}{2k_B T}\right)\right]. \tag{20}$$

In Eq. (20) $\Delta(T)$ is the BCS-energy gap, $R_{n\square}$ the normal state sheet resistance of the film and R_u the universal resistance $\hbar/e^2$. Since μ is a function of $n_\square$, equation (18) shows that T_{LU} depends upon the matching configuration under considera-

tion. For a triangular lattice such configurations are defined by [8]

$$B_{n_1 n_2} = \frac{\sqrt{3}}{2} \frac{\phi_0}{\lambda_g^2} (n_1^2 + n_2^2 + n_1 n_2)^{-1}, \tag{21}$$

where n_1 and n_2 are integers. Then, in the limit of low sheet resistances $R_{n\square} \ll R_u$ from equations (18) – (21) one obtains for the transition temperature T_{LU} of the fundamental matching configuration $\vec{q} = \vec{g}_1$ $(n_1 = 1,\ n_2 = 0)$

$$\frac{T_{LU}}{T_c} = 1 - 0.31 \frac{R_{n\square}}{R_u}, \tag{22}$$

where T_c is the BCS-transition temperature of the film. The LU-transition temperatures corresponding to configurations defined by higher values of n_1 and n_2 lie below that given by equation (22).

The case of finite mismatch ($\delta \neq 0$) is more delicate. It has been recently studied in a slightly different context (the 2D classical sine–Gordon system) by Puga et al. [12] using a renormalization-group approach, where, for the first time, δ is considered as a new renormalizable parameter. Although several aspects of the LU-transition emerging from their calculation turn out to be quite different from those following from the much simpler SCHA-scheme, the shape of the phase boundary $\delta_c(T)$ resulting from their approach is very similar to that predicted by SCHA. In the latter approximation $\delta_c(T)$ simply follows from equation (8) by replacing Δ with its renormalized value Δ_R given by equation (17). The resulting phase diagram is shown in Fig. 5, where, instead of $\delta_c(T)$, we have

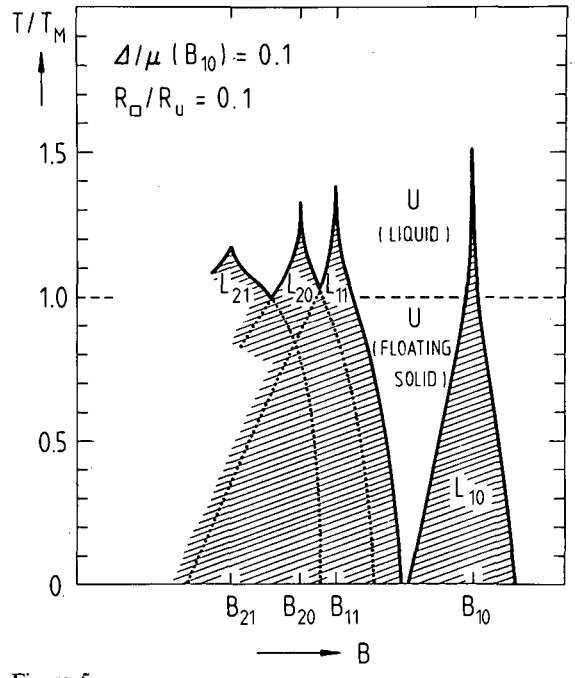

Figure 5
Phase diagram in the (B, T)-plane of a 2D vortex lattice interacting with a 1D periodic potential.

plotted the related quantity $B_c(T) = B_{n_1 n_2}[1 - \delta_c(T)]^2$. Since, for convenience, B_c is reported on a logarithmic scale, the phase boundary delimiting a given L-phase, which would be symmetric about $B_{n_1 n_2}$ on a linear plot, appear asymmetrical. Assuming Δ independent of B, in constructing Fig. 5 Δ/μ was kept constant, for simplicity, within each of the different L-phases, but was scaled according to equations (19) and (21) from L-phase to L-phase. In Fig. 5 temperatures are conveniently measured in units of T_M, the melting temperature of the 2D vortex lattice [5–7], which, as shown by the following equation, is independent of B at moderate vortex densities

$$k_B T_M = \frac{1}{4\pi}\mu(T_M)a^2. \tag{23}$$

With this additional aspect of the problem in mind, it is argued that, if the LU-transition takes place for $T > T_M$, it is a transition from a solid L-phase to a fluid-like U-phase. This is the case for the L-phases of lower order (n_1 and n_2 small) of Fig. 5, where T_{LU} is larger than T_M. With a straightforward calculation based on equations (18), (21) and (23) it can be shown, however, that there is a particular commensurate phase, the L_{22}-phase, for which T_{LU} becomes equal to T_M. For L-phases of higher order T_{LU} is always lower than T_M and, consequently, the LU-transition is from a solid epitaxial L-phase to a solid floating U-phase.

III. Critical currents

To test some of the theoretical ideas put forward in the previous section, critical current (I_c) measurements were performed on thickness modulated granular Al-films as a function of magnetic field and temperature. A combined holographic photolithographic technique was used to fabricate grating-like film profiles with $\lambda_g \lesssim 1\ \mu m$. To meet the condition, $\Delta < \mu$, for weak pinning, the relative thickness modulation $\Delta d/d$ was kept below ~20–25%. The most relevant superconducting and normal state properties of the two Al-films studied in this paper are summarized in Table 1.

Since a registered L-phase is pinned by the periodic film structure, a finite force is required to depin the vortex lattice and, subsequently, to sustain vortex motion in the dissipative flux-flow régime. In our experiments such a force is provided by a uniform transport current flowing parallel to the grooves of the grating-like film profile. A U-phase, on the other hand, is not pinned by the periodic substrate, its energy being independent, at least within the framework of

Table 1

Film	d[Å]	$\Delta d/d$[a]	$\lambda_g[\mu m]$	$R_{n\square}[\Omega]$	T_c[K]	$(\xi_0 l)^{1/2}$[Å][b]	$\lambda_L(0)\left(\frac{\xi_0}{l}\right)^{1/2}$[Å][b]
Al1	200	~0.2	0.79	15	1.89	365	4300
Al2	200	~0.2	0.77	35	2.16	223	6140

[a] Determined by combined optical and electrical methods.
[b] Calculated using $\rho l = 4 \times 10^{-12}\ \Omega\,cm^2$ and $\lambda_L(0) = 157$ Å for Al. ξ_0 was scaled from the bulk Al value (1, 6 μm) according to our T_c.

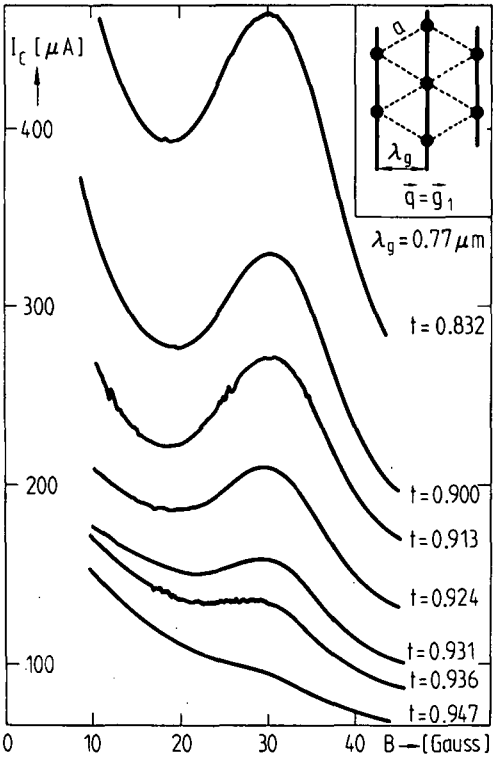

Figure 6
Critical current vs. magnetic field curves of a thickness modulated film (Al2) for different reduced temperatures $t = T/T_c$.

the continuum approximation, of the relative position of the vortex lattice with respect to the pinning potential. Therefore, the critical current for entering the flux-flow régime vanishes in this case.

In Fig. 6 $I_c(B)$-curves of the film Al2 are shown for different temperatures. One can easily verify, using equation (21), that the peak at $B \approx 30$ gauss is the signature of the fundamental L_{10}-configuration shown in the insert of Fig. 6. According to our previous discussion, the width of this peak, taken in the limit of vanishing critical current, is a measure of the critical mismatch $\delta_c(T)$ and, consequently, could in principle be used to determine the $L_{10}U$-phase boundary. For two reasons, however, this appears to be, in practice, a problem of difficult solution. The first and most important one is that in our films, as we shall show later on, Δ is of the order of μ, typically $\Delta/\mu \approx 0.9$. Under this condition considerable overlapping of the L_{10}-phase with the L_{11}-phase is expected (in Fig. 5 overlapping of the different L-phases is enhanced as Δ/μ increases). This is at the origin of the relatively high shoulder on the low field side of the I_c-peak in Fig. 6. Additional evodence for substantial overlapping effects is also provided by the fact that the L_{11} and L_{20}-configurations were hard to resolve in our experiments. The second reason is that in real films one is dealing with unavoidable

pinning effects due to randomly distributed inhomogeneities, which result in a finite contribution to I_c even in the U-phase. Clearly, both overlapping and random pinning effects render a determination of the peak width quite uncertain. In the rest of the paper, therefore, we shall concentrate on a much more accessible experimental quantity: the temperature dependent strength $I_{cM}(T)$ of a critical current peak.

For perfect matching the equilibrium position of a vortex is determined [13, 14] by balancing the Lorentz driving force $\vec{F}_L = d(\vec{j} \times \vec{\phi}_0)$ against the pinning force experienced by the vortex in the effective cosine-potential $\Delta_R'(1-\cos q\phi)$, where $\Delta_R' = \Delta_R/n_\square$. This results in the following expression for the transport current density

$$j = \frac{q\Delta_R'}{\phi_0 d} \sin \Phi \tag{24}$$

Obviously, the critical current density j_{cM} is reached for $\Phi = \pi/2$, a condition corresponding to vortices located halfway between the bottom and the top of the potential wells. Thus, using equation (17), j_{cM} can be written as

$$j_{cM} = \frac{q\Delta'}{\phi_0 d} \left(\frac{\Delta}{\mu}\right)^{T/(T_{LO}-T)}. \tag{25}$$

In order to analyse our I_c-data with equation (25) we need a model for Δ' (or Δ), the characteristic energy scale of the pinning mechanism operating in our thickness modulated films. In the thin film limit ($d \ll \lambda$) the potential energy $\varepsilon(\vec{r})$ of a vortex located at $\vec{r}$ can be expressed by the convolution [15]

$$\varepsilon(\vec{r}) = \int f(\vec{r}' - \vec{r})\, d(\vec{r}')\, d^2r', \tag{26}$$

where $d(\vec{r}') = d + \Delta d \cos qx$ is the thickness modulation and $f(\vec{r}' - \vec{r})$ the free energy density distribution within the flux line. There are three major contributions to f: an electromagnetic contribution f_{em} arising from the field and supercurrent distributions in the vortex, a contribution f_k representing the kinetic energy cost to produce the vortex and a contribution f_c due to the condensation energy paid in creating its normal core. In our case f_{em} is expected to contribute very little to the integral in equation (26), its characteristic scale of variation, the effective penetration depth Λ, being much larger than λ_g ($q\Lambda \gg 1$). Varying over distances of the order of the coherence length ξ, which is much smaller than λ_g in the temperature region of interest here, f_k and f_c provide the dominant contributions to ε. Using Clem's model [16] for f_k and f_c, from equation (26) one obtains in the limit $q\xi < 1$ and of large GL-parameters $\kappa = \lambda/\xi$

$$\varepsilon(x) \approx 2(\Delta d/d)(\phi_0/4\pi)^2 \frac{1}{\Lambda}(1+\cos qx). \tag{27}$$

Accordingly, Δ is identified as

$$\Delta \approx 2n_\square(\Delta d/d)(\phi_0/4\pi)^2 \frac{1}{\Lambda}. \tag{28}$$

This expression shows that Δ has the same temperature dependence as μ, a

considerable simplification in the analysis of the I_c-data. By combining equations (25) and (28), I_{cM} can finally be written in the form

$$\frac{I_{cM}(T)}{I_{cM}(0)} = \frac{\Lambda(0)}{\Lambda(T)} \left(\frac{\Delta}{\mu}\right)^{T/T_{LU}-T)} \tag{29}$$

where $\Delta/\mu \approx 4(\Delta d/d)$. This result shows very clearly that with rising temperature thermal fluctuations further reduce $I_{cM}(T)$ with respect to the "BCS"-value $I_{cM}(T) = I_{cM}(0)\,[\Lambda(0)/\Lambda(T)]$. After substraction of the background due to random pinning, which was deduced from a flat but otherwise identical reference film, the critical currents $I_{cM}(T)$ of Al1 and Al2 were fitted to equation (29) using $I_{cM}(0)$, Δ/μ and T_{LU}/T_c as fitting parameters. The result of this analysis is shown in Fig. 7 where, for comparison, theoretical curves calculated by neglecting the effect of thermal fluctuations are also shown. Good agreement with equation (29) is found for a reasonable choice of the parameters. T_{LU}/T_c, in fact, scales with $R_{n\square}$ approximately as predicted by equation (22) where, however, the numerical coefficient (0.31) is found to be about an order of magnitude too small to account for the experimental values of Fig. 7. At the present stage of our investigations, however, it is not possible to attribute this discrepancy to an intrinsic weakness of

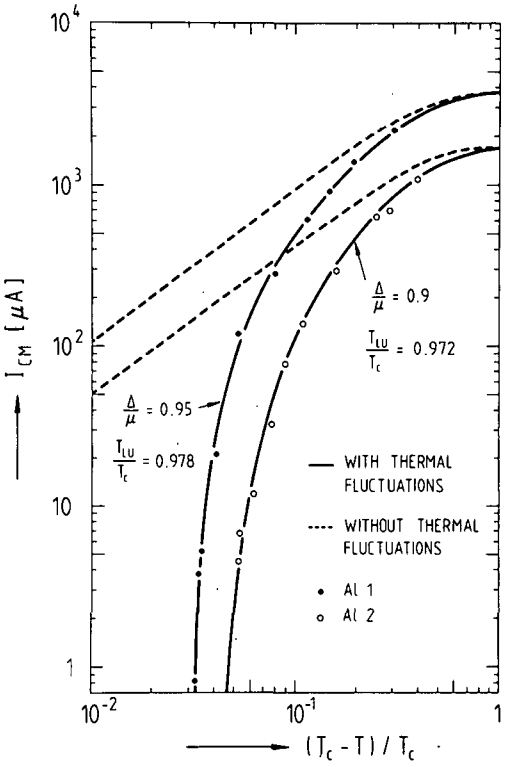

Figure 7
Temperature dependence of the critical currents of thickness modulated films for the fundamental matching configuration $\vec{q} = \vec{g}_1$. Theoretical curves are calculated from equation (29) with (full lines) and without (dashed lines) the effect of thermal fluctuations.

the model discussed in Section II.B. As for Δ/μ, there is good agreement between the values deduced from the fit and those estimated with $\Delta/\mu \approx 4(\Delta d/d)$ using values of $\Delta d/d$ (see Table 1) determined by combined optical and electrical methods. On the basis of these results, we conclude that the concept of a pinning force field renormalized by thermal fluctuations provides a good description of our experiments.

Acknowledgments

In writing this contribution to a volume dedicated to J. L. Olsen in honour of his 60th birthday, one of us (P.M.) would like to express to him his deep gratitude for the exciting years he spent working under his stimulating guidance, for his friendship and for his generosity.

We thank M. Puga for valuable discussions. This work has been supported by the Swiss National Science Foundation.

REFERENCES

[1] O. Daldini, P. Martinoli, J. L. Olsen and G. Berner, Phys. Rev. Lett. *32*, 218 (1974).
[2] P. Martinoli, H. Beck, M. Nsabimana and G. A. Racine, Physica *107B*, 455 (1981).
[3] For a review see, e.g., J. Villain, in *Ordering in Two Dimensions*, edited by S. K. Sinha (North Holland, New York, 1980), p. 123.
[4] V. L. Pokrovsky and A. L. Talapov, Phys. Rev. Lett. *42*, 65 (1979); Zh. Eksp. Teor. Fiz. *78*, 269 (1980) [Sov. Phys. JETP *51*, 134 (1980)].
[5] J. M. Kosterlitz and D. J. Thouless, J. Phys. C *6*, 1181 (1973).
[6] B. A. Huberman and S. Doniach, Phys. Rev. Lett. *43*, 950 (1979).
[7] D. R. Nelson and B. I. Halperin, Phys. Rev. B *19*, 2457 (1979).
[8] P. Martinoli, Phys. Rev. B *17*, 1175 (1978).
[9] A. T. Fiory, Phys. Rev. B *8*, 5039 (1973).
[10] F. C. Frank and J. H. van der Merwe, Proc. R. Soc. (London), Ser. A, *198*, 205 (1949).
[11] M. Tinkham, *Introduction to Superconductivity* (McGraw-Hill, New York, 1975), p. 80.
[12] M. W. Puga, E. Simanek and H. Beck, Phys. Rev. B *26*, 2673 (1982).
[13] P. Martinoli, J. L. Olsen and J. R. Clem, J. Less-Common Metals *62*, 315 (1978).
[14] P. Martinoli and J. R. Clem, in *Inhomogeneous Superconductors*, edited by T. L. Francavilla, D. V. Gubser, J. R. Leibowitz and S. A. Wolf (AIP,New York, 1980), AIP Conf. Proc. No *58*, 176 (1980).
[15] A. Schmid and W. Hauger, J. Low Temp. Phys. *11*, 667 (1973).
[16] J. R. Clem, J. Low Temp. Phys. *18*, 427 (1975) and unpublished work.

From: PERCOLATION, LOCALIZATION,
AND SUPERCONDUCTIVITY
Edited by Allen M. Goldman
and Stuart A. Wolf
(Plenum Publishing Corporation, 1984)

STATIC AND DYNAMIC PROPERTIES OF COMMENSURATE AND INCOMMENSURATE PHASES OF A TWO-DIMENSIONAL LATTICE OF SUPERCONDUCTING VORTICES

P. Martinoli, H. Beck, M. Nsabimana and G.A. Racine

Institut de Physique, Université de Neuchâtel
CH - 2000 Neuchâtel, Switzerland

INTRODUCTION

Phase transitions in two-dimensional (2D) systems have received considerable attention recently. In several experiments the 2D crystal under consideration is exposed to the force field created by a periodic substrate. Among other situations this is the case of a 2D lattice of superconducting vortices interacting with a periodic pinning potential. As pointed out by Martinoli and coworkers[1-3] some years ago, thin superconducting films, whose thickness is periodically modulated in one dimension, provide such a system. In this lecture we discuss the static and dynamic behaviour of this model system in which the 2D vortex lattice can be driven through a variety of phases[4,5] simply by changing the conditions of flux-line density and/or temperature. In particular, we show how measurements of the critical currents and of the complex rf impedance of thickness-modulated layers can be used to probe the transition of the 2D vortex lattice from a "locked" commensurate (C) phase in registry with the substrate periodicity to a "floating" incommensurate (I) solid phase exhibiting 2D topological order[6,7] or to a fluid-like phase.

THE PHASE DIAGRAM

The phase diagram of 2D crystals interacting with a periodic force field has been studied by a number of authors[4,5]. It is determined by considering, in addition to phonons, two types of topological excitations: domain walls (also called discommensurations,

kinks, or solitons) which trigger the instability of a C-phase with respect to an I-phase (CI-transition) and dislocations which drive melting of the floating-solid phase (I-phase) into a liquid-like phase through the dislocation unbinding mechanism proposed by Kosterlitz and Thouless[6,7].

Dealing with situations where the periodic substrate is, as in our case, anisotropic, a recent theory by Pokrovsky and Talapov[8] (PT) is particularly relevant for the understanding of our experiments, where the 2D vortex lattice experiences the 1D periodic pinning potential created by the thickness modulation. In the following we review some of the basic concepts and results of the PT-theory. The only important difference between our treatment and the one by PT is that in establishing the CI-phase boundary we use, instead of their renormalization-group technique, an alternative approach based on the more transparent *S*elf-*C*onsistent *H*armonic *A*pproximation (SCHA) obtaining a similar result[9,10]. The modifications of the phase diagram resulting from the presence of thermally excited dislocations, which are not included in the PT-model, are briefly discussed at the end of this section.

The CI-Transition at Zero Temperature

We consider a 2D triangular lattice of superconducting vortices, with lattice parameter a, in static interaction with a 1D harmonic potential of amplitude Δ and wave vector $\vec{q}$ ($q = 2\pi/\lambda_q$). We focus our attention on situations where $\vec{q}$ is very close to one of the vectors, $\vec{g}$, of the reciprocal vortex lattice, the condition $\vec{q} = \vec{g}$ defining a configuration of perfect matching between the (undistorted) lattice and the sinusoidal pinning potential. It is assumed that the flux-line lattice is incompressible and, further, that the pinning is weak when compared to the lattice stiffness, i.e. $\Delta < \mu$, where μ is the shear modulus of the vortex lattice[11]. Under these conditions only long-wavelength shear deformations turn out to be relevant and, as a consequence, the vortex lattice can be treated as an elastic continuum. Then, the energy $\mathcal{E}$ of the system can be written as the sum of an elastic contribution due to the pinning-induced lattice distortions and of a potential energy contribution due to the periodic pinning field :

$$\mathcal{E} = \int \left[\frac{\mu}{2}\left(\frac{\partial u}{\partial y} + \frac{\partial v}{\partial x}\right)^2 + \Delta(1 - \cos q\phi)\right] dx\, dy \,. \qquad (1)$$

In writing this expression we have jumped ahead to the conclusion of PT asserting that, at $T \approx 0$, the ground state of the system is characterized by a quasi 1D deformation field $\vec{w}$, whose components (u,v) in an $(x\text{-}y)$-reference frame with x pointing in a direction

forming an angle of 45^0 with $\vec{q}$ are given by :

$$u = \delta y , \qquad v = \delta x - \sqrt{2}\,\phi(x) , \tag{2}$$

where $\delta = 1 - (g/q)$ measures the degree of mismatch. It clearly emerges from these expressions that $\vec{w}$ results from the superposition of two uniform shear deformations (one along x and the other along y) and of a 1D transverse field $\phi(x)$ which, for an incompressible lattice, is found to propagate along x[3,8]. In an (x'-y')-coordinate system rotated by 45^0 with respect to (x-y) the uniform part of $\vec{w}$ is an area conserving deformation consisting of a uniform compression ($\delta > 0$) or expansion ($\delta < 0$) - $\delta x'$ along x' (parallel to $\vec{q}$) combined with a uniform expansion ($\delta > 0$) or compression ($\delta < 0$) $\delta y'$ along y'. This uniform deformation is such that the potential energy contribution to $\mathcal{E}$ vanishes : the vortices are forced to lie at the bottom of the potential wells of the cosine-potential.

To determine $\phi(x)$, we simply minimize the functional $\mathcal{E}[\phi(x)]$ with respect to $\phi(x)$, thereby obtaining the following sine-Gordon equation[12] for the "phase" field $\Phi(x) = q\phi(x)$:

$$\sin\Phi - \ell^2 \frac{\partial^2\Phi}{\partial x^2} = 0 , \tag{3}$$

where $\ell^2 = 2\mu/\Delta q^2$. Its solution in terms of elliptic functions

$$\Phi(x) = \pi + 2\mathrm{am}(x/k\ell) \tag{4}$$

is a stair-shaped function representing a regular sequence of kinks, whose period L is related to k by

$$L = 2k\ell K(k) , \tag{5}$$

where K(k) is a complete elliptic integral of the first kind. Using Eqs. (4) and (5), $\mathcal{E}$ can be expressed as a function of the variational parameter k. Then, minimization of $\mathcal{E}(k)$ with respect to k leads to :

$$|\delta| = (2/\pi)(\Delta/\mu)^{1/2}[E(k)/k] , \tag{6}$$

where E(k) is a complete elliptic integral of the second kind. There are solutions of Eq. (6) satisfying the condition $0 \leq k \leq 1$ only if $|\delta|$ is larger than a critical mismatch δ_c given by :

$$\delta_c = (2/\pi)(\Delta/\mu)^{1/2} \tag{7}$$

For $|\delta| > \delta_c$ $\Phi(x)$ is of the form (4). As a consequence, for $|\delta| > \delta_c$ the vortex lattice is characterized by the formation of a

superstructure, of period L, consisting in a regular 1D sequence of domain walls propagating at 45° with respect to $\vec{q}$. This is the incommensurate I-phase shown in Fig. 1. In constructing this figure we have assumed that the starting matching configuration is that defined by $\vec{q} = \vec{g}_{10}$, $\vec{g}_{10}$ being one of the six nearest-neighbour reciprocal lattice vectors ($g_{10} = 4\pi/a\sqrt{3}$). Since $\delta > 0$, large portions of the lattice shown in Fig. 1 appear to be uniformly compressed along x' and expanded along y' and are essentially commensurate to the underlying 1D periodic substrate. These regions are separated from each other by discommensurations where the phase field $\Phi(x)$, which is essentially constant in the nearly commensurate regions between successive kinks, changes by 2π over distances of the order of $\sim k\ell$. The period L of the superstructure diverges logarithmically as $|\delta|$ approaches δ_c [$k \to 1$ in Eq. (5)].

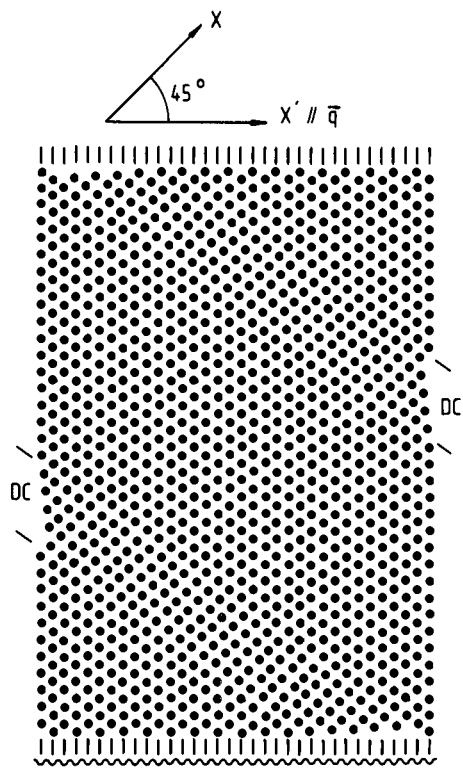

Fig. 1. Incommensurate I-phase for $\delta = 0.13$ ($B/B_{10} = 0.76$). Discommensurations (DC) form a periodic 1D sequence propagating along the x-direction.

For $|\delta| < \delta_c$ there are no solutions of Eq. (6) and, consequently, $\Phi(x)$ is no longer given by Eq. (4). In this case $\mathcal{E}$ has its minimum value when the potential energy contribution due to the periodic pinning field vanishes in Eq. (1), i.e. when $\Phi(x) = 0$ everywhere. This, of course, corresponds to the commensurate C-phase shown schematically in Fig. 2 for $\delta = 0$ (matching configuration $\vec{q} = \vec{g}_{10}$) and for vortex densities corresponding to deviations from perfect registry but still such that $|\delta| < \delta_c$.

The areal free energy density $F_\square$ of the 2D vortex lattice can be written in the form :

$$F_\square = 2\mu\delta^2 - 2\Delta\{[\delta/\delta_c E(k)]^2 - 1\}\,\theta(|\delta| - \delta_c)\,, \qquad (8)$$

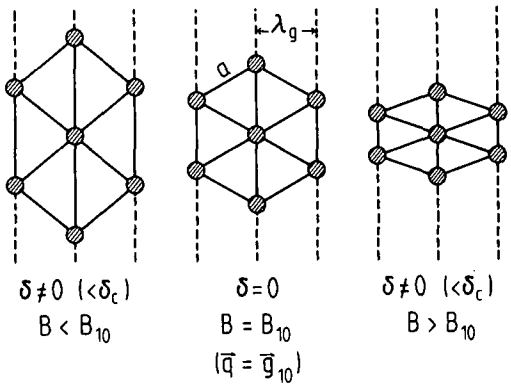

Fig. 2. The fundamental commensurate C_{10}-phase in three different states of deformation.

where $\theta(z)$ is the Heaviside step-function. The first term on the right-hand side of Eq. (8) is the elastic energy density associated with the uniform deformation appearing in both the C- and the I-phase, whereas the second one is due to the phase field $\Phi(x)$ and therefore contributes to $F_\square$ only in the I-phase.

Phase Transitions at Finite Temperatures

To study the CI-transition at finite temperatures, we first consider the case of perfect matching ($\delta = 0$), which is particularly simple. For $\vec{q} = \vec{g}$ the vortices execute a Brownian motion around the equilibrium positions they would assume at the bottom of the potential wells at T = 0. Accordingly, the Langevin equation of motion for a vortex at the lattice site $\underline{l}$ can be written as :

$$\eta \dot{\vec{u}}_{\underline{l}} = - \sum_{\underline{l}'}{}' \tilde{G}(\underline{l} - \underline{l}')\vec{u}_{\underline{l}'} - \vec{q}\Delta' \sin(\vec{q} \cdot \vec{u}_{\underline{l}}) + \vec{f}_{\underline{l}}(t) , \qquad (9)$$

where the four terms represent, successively, the viscous damping force, the lattice restoring force, the sinusoidal pinning force and the fluctuating Langevin force acting on the vortex at $\underline{l}$. $\eta^{-1} = R_{\square}/B\phi_0$, where $R_{\square}$ is the sheet flux-flow resistance of the superconducting film, is the mobility[13] of a free vortex, $\tilde{G}(\underline{l} - \underline{l}')$ the elastic matrix and Δ' is related to Δ by $\Delta = n_{\square}\Delta'$, where $n_{\square} = B/\phi_0$ is the areal vortex density. $\vec{f}_{\underline{l}}(t)$ is assumed to have a white noise spectrum defined by the correlation function :

$$\langle f_{\underline{l}\alpha}(t) f_{\underline{l}'\beta}(t') \rangle = 2\eta k_B T \delta_{\alpha\beta} \delta_{\underline{l}\underline{l}'} \delta(t - t') , \qquad (10)$$

stating that the Langevin force is uncorrelated in direction, space and time. To find the mean square fluctuation $\langle u^2 \rangle$ of the vortices, which is the quantity of interest here, it is convenient to expand $\vec{u}_{\underline{l}}(t)$ in normal modes of the vortex lattice[10]. Then, linearizing Eq. (9) within the framework of SCHA and considering, as before, only transverse (t) modes of the lattice the following expression for the t-component of the normal mode amplitude $\vec{u}_{\underline{k}}(\omega)$ is obtained :

$$u_{\underline{k}t}(\omega) = \frac{n_{\square} f_{\underline{k}t}(\omega)}{D_{\underline{k}t} + \Delta_R (\vec{q} \cdot \hat{e}_{\underline{k}t})^2 - i\eta\omega} , \qquad (11)$$

where $D_{\underline{k}t}$ is the matrix element of the (diagonal) dynamical matrix associated with t-modes, $\hat{e}_{\underline{k}t}$ the polarization vector for t-deformations and $f_{\underline{k}t}(\omega)$ the t-Fourier component of the Langevin force. In our SCHA-approach the effective strength, Δ_R, of the pinning field experienced by the vortices is given by :

$$\Delta_R = \Delta \, e^{-\frac{1}{2} q^2 \langle u_{tx}^2 \rangle} , \qquad (12)$$

where $\langle u_{tx}^2 \rangle$ is the mean square t-fluctuation along the x-direction parallel to $\vec{q}$. Therefore, in our treatment the renormalization

effect of the thermal fluctuations, which provides the essential mechanism for the phase transition, enters through a Debye-Waller factor which weakens the periodic pinning force acting on the vortices. To calculate the mean square t-fluctuation $\langle u_t^2 \rangle$ we assume a Debye model, for which $D_{\underline{k}t} = \mu k^2$, and replace the required sum over $\underline{k}$ by an integral over a smooth density of states. Then, in the weak pinning limit $\Delta << \mu$ considered here we deduce from Eqs. (10) and (11) :

$$\langle u_t^2 \rangle = \frac{k_B T}{4\pi\mu} \ln(\mu/\Delta_R) \, . \tag{13}$$

This result shows quite clearly that in a C-phase the vortex lattice is a 2D solid with conventional long-range order as long as Δ_R remains finite. As expected for 2D systems, $\langle u_t^2 \rangle$ diverges logarithmically as Δ_R vanishes. Since, by equipartition, $\langle u_{tx}^2 \rangle \approx (1/2)\langle u_t^2 \rangle$ in the limit $\Delta << \mu$, from Eqs. (12) and (13) one deduces :

$$\Delta_R/\Delta = (\Delta/\mu)^{T/(T_{LU} - T)} \, , \tag{14}$$

where T_{LU} is implicitly given by :

$$k_B T_{LU} = (4/\pi)\mu(T_{LU})\lambda_g^2 \, . \tag{15}$$

It clearly emerges from Eq. (14) that at the "*L*ocking-*U*nlocking" temperature T_{LU} the vortex lattice undergoes a transition from a perfectly matched ($\delta = 0$) "locked" C-phase ($\Delta_R \neq 0$) to an "unlocked" phase ($\Delta_R = 0$) whose precise nature (floating solid or liquid) will be discussed in a moment. It should be noticed that the expression for T_{LU} deduced with our SCHA-scheme is the same as that obtained by PT using a renormalization-group technique.

For a moderately dense lattice of vortices in dirty superconducting films μ can be written in the form[11] :

$$\mu(T) = (1/2) n_{\square} (\phi_o/4\pi)^2 \Lambda^{-1}(T) \, , \tag{16}$$

where $\Lambda = 2\lambda^2/d$ is the effective penetration depth for 2D superconducting layers[10,14]. Since μ is a function of $n_{\square} = B/\phi_o$, Eq. (15) shows that T_{LU} depends upon the matching configuration under consideration. For a triangular lattice such configurations are defined by[3] :

$$B_{mn} = (\sqrt{3}/2)(\phi_o/\lambda_g^2)(m^2 + n^2 + mn)^{-1} \, , \tag{17}$$

where m and n are integers. Expressing $\Lambda(T)$ in terms of the normal state sheet resistance $R_{n\square}$ of the film, the transition temperature T_{LU} for the fundamental C_{10}-phase (m = 1, n = 0 corresponding to $\vec{q} = \vec{g}_{10}$) deduced from Eqs. (15) and (16) can be written in the form :

$$T_{LU}/T_c \approx 1 - 0.31(R_{n\square}/R_u) \quad \text{for} \quad R_{n\square} << R_u , \tag{18}$$

where T_c is the BCS-transition temperature and R_u the universal sheet resistance $\hbar/e^2$. LU-transition temperatures for C_{mn}-phases defined by higher values of m and n lie below that given by Eq. (18).

The case of finite mismatch ($\delta \neq 0$) is more delicate. It is clear, however, that, as a consequence of the fluctuating Brownian motion of the vortices, the critical degree of mismatch $\delta_c(T)$ tolerated by a C-phase becomes smaller and smaller as the temperature rises and finally vanishes at $T = T_{LU}$. PT determined the phase boundary $\delta_c(T)$ using a renormalization-group technique, in which the only renormalizable parameter is the pinning potential amplitude Δ[8]. More recently, Puga et al.[15,16] have generalized the PT-treatment by considering the effect of renormalization also on μ and δ. Although several aspects of the CI-phase transition emerging from their calculation turn out to be different from those following from the much simpler SCHA-scheme, the shape of the phase boundary $\delta_c(T)$ resulting from their approach is very similar to that predicted by SCHA. In the latter approximation $\delta_c(T)$ simply follows from Eq. (7) by replacing Δ with its renormalized value Δ_R given by Eq. (14). The resulting phase diagram is shown in Fig. 3, where, instead of $\delta_c(T)$, we have plotted the related quantity $B_c(T) = B_{mn}[1 \pm \delta_c(T)]^2$. Temperatures are conveniently measured in units of T_M, the melting temperature of the 2D vortex lattice[17,18], which, as shown by Eq. (16) and the following equation, is independent of B at moderate vortex densities :

$$k_B T_M = (1/4\pi)\mu(T_M)a^2 . \tag{19}$$

So far, only domain wall excitations, which drive the CI-phase transition, have been included in our analysis. To obtain the complete phase diagram, however, several authors[7,10,19-25] have emphasized that it is necessary to add the effect of thermally excited dislocation pairs[6,7] in order to assess the stability of the I-phase against melting into a fluid-like phase. Recently, Haldane et al.[26] have given a rather unified description of the phase diagram showing that it strongly depends on the order of commensurability p, which for our triangular lattice is related to m and n by $p = (2/\sqrt{3})(m^2 + n^2 + mn)^{1/2}$. For $p < \sqrt{8}$ they find that,

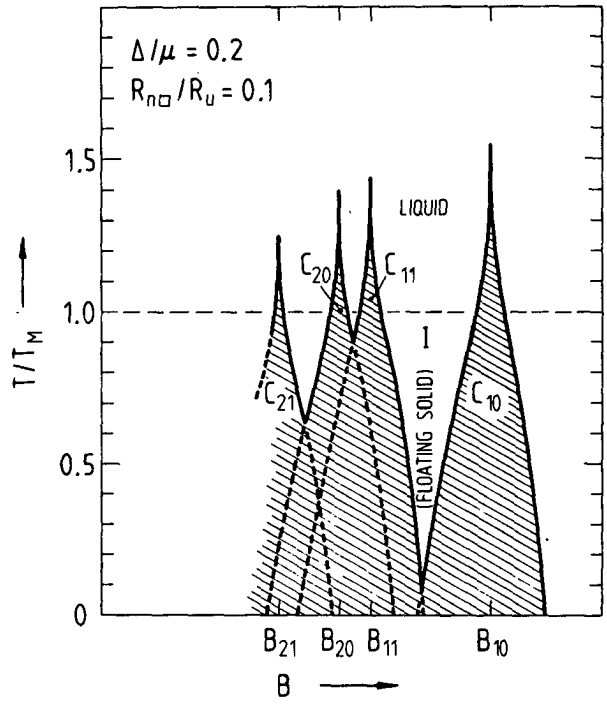

Fig. 3. Phase diagram in the (B,T)-plane of a 2D vortex lattice in a 1D periodic potential.

at finite temperatures, there is always a liquid phase separating the C-phase from the I-phase, whereas for $p > \sqrt{8}$ a direct CI-phase transition is always possible. Although important for a deeper understanding of the physics of 2D system, these features play only a marginal role in the analysis of the experiments reported later on in this lecture. Thus, for simplicity, in constructing the phase diagram of Fig. 3 we have assumed that, in the I-phase, the vortex lattice is a 2D floating solid undergoing a melting transition driven by the unbinding of dislocation dipoles at $T = T_M$. It follows that, if the CI-transition occurs for $T > T_M$, it is actually a transition from a C-phase to a fluid-like phase. This is the case for the lower order C-phases of Fig. 3, where T_{LU} is larger than T_M. A straightforward calculation based on Eqs. (15), (17) and (19) shows, however, that there is a particular commensurate phase, the C_{22}-phase corresponding to $p = 4$, for which T_{LU} becomes equal to T_M. For C-phases of higher order ($p > 4$) T_{LU} is always lower than T_M

and, consequently, a floating solid phase always separates the C-phase from the liquid phase. This agrees with the findings of other authors[19,20,22,23,26].

CRITICAL CURRENTS

To test some of the theoretical ideas put forward in the previous section, critical current (I_c) measurements were performed on thickness modulated granular Al-films as a function of magnetic field and temperature. A combined holographic-photolithographic technique[1] was used to fabricate grating-like film profiles with $\lambda_g \lesssim 1$ μm and with a relative thickness modulation, $\Delta d/d$, less than 20 - 25%. The most relevant superconducting and normal state parameters of the two Al-films studied in this work are summarized in Table 1.

Since a registered C-phase is pinned by the periodic film structure, a finite current, flowing parallel to the 1D grooves, is required to depin the vortex lattice and, subsequently, to sustain vortex motion in the dissipative flux-flow régime. An I-phase, on the other hand, is not pinned by the periodic substrate, its energy being independent of the relative position of the discommensurations with respect to the pinning potential. Therefore, the critical current for entering the flux-flow régime vanishes in this case.

In Fig. 4 $I_c(B)$-curves for the film Al*1* are shown for different reduced temperatures $t = T/T_c$. Using Eq. (17), one can easily verify that the peak at $B \approx 28$ Gauss corresponds to the fundamental C_{10}-configuration ($p = 2/\sqrt{3}$) shown in Fig. 2, while the small structure at $B \approx 7$ Gauss can be assigned to the C_{11}- and C_{20}-phases which, on account of their strong overlap (see Fig. 3), are hard to resolve from each other. The shape of the $I_c(B)$-peak associated with a given C-phase has been calculated by Burkov and Pokrovsky[27]. In

Table 1. Parameters of the Al-Films

Film	d[Å]	$\Delta d/d$[a]	λ_g[μm]	$R_{n\square}$[Ω]	T_c[K]	$(\xi_0 l)^{1/2}$[Å][b]	$\lambda_L(0)\left(\frac{\xi_0}{l}\right)^{1/2}$[Å][b]
Al1	200	~0.2	0.79	15	1.89	365	4300
Al2	200	~0.2	0.77	35	2.16	223	6140

a Determined by combined optical and electrical methods.
b Calculated using $\rho l = 4 \times 10^{-12}\,\Omega\,\mathrm{cm}^2$ and $\lambda_L(0) = 157$ Å for Al. ξ_0 was scaled from the bulk Al value (1,6 μm) according to our T_c.

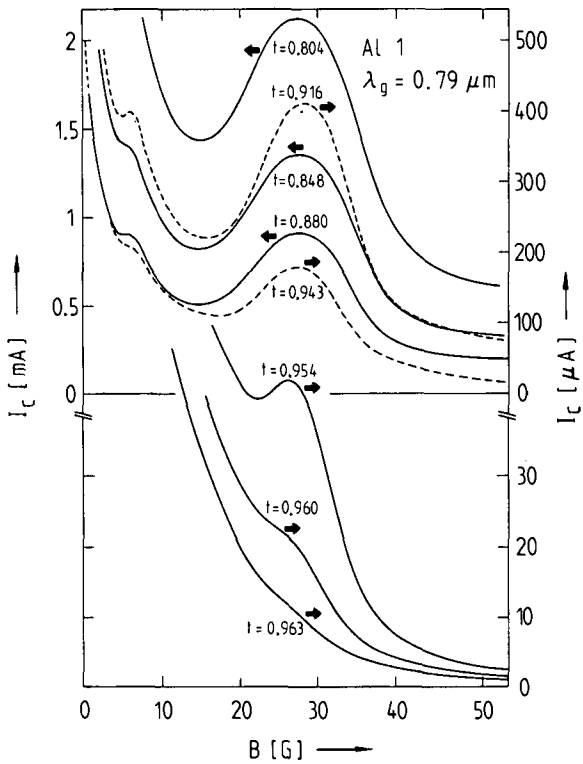

Fig. 4. Critical current vs. magnetic field curves of a thickness modulated film (Al1) at different reduced temperatures $t = T/T_c$.

a sample of finite size it is determined by the stability of the C-phase against the nucleation of a domain wall at the boundary of the film. Therefore, a detailed comparison of the shape of the main peak in Fig. 4 with the theoretical prediction of this model could, in principle, allow a determination of the C_{10}I-phase boundary. For two reasons, however, this appears to be, in practice, a difficult problem. The first and more important one is that in our films Δ is found to be of the order of μ, typically $\Delta/\mu \approx 0.9$. Under this condition one expects considerable overlap of the C_{10}-phase with the C_{11}-phase (in Fig. 3 the overlap of the various C-phases is enhanced as Δ/μ increases). This is certainly at the origin of the relatively high shoulder on the low field side of the fundamental I_c-peak in Fig. 4. The second reason is that in real films one is

dealing with unavoidable pinning effects due to randomly distributed inhomogeneities, which result in a finite contribution to I_c even in the I-phase. Clearly, both overlapping and random pinning effects render the analysis of the peak shape quite difficult. We shall therefore concentrate on a much more accessible experimental quantity : the temperature dependent strength $I_{cM}(T)$ of a critical current peak.

For perfect matching the equilibrium position of a vortex is determined[3,28,29] by balancing the Lorentz driving force $\vec{F}_L = d\phi_o(\vec{j} \times \hat{z})$ against the pinning force experienced by the vortex in the effective cosine-potential $\Delta_R'(1 - \cos q\phi)$. This results in the following expression for the transport current density :

$$j = (q\Delta_R'/\phi_o d)\sin\Phi \, . \tag{20}$$

The critical current density, j_{cM}, is reached for $\Phi = \pi/2$, a condition corresponding to vortices located halfway between the bottom and the top of the potential wells. Thus, using Eq. (14) j_{cM} can be written as :

$$j_{cM} = (q\Delta'/\phi_o d)(\Delta/\mu)^{T/(T_{LU} - T)} \, . \tag{21}$$

In order to compare our I_c-data with Eq. (21) we need a model for $\Delta = n_\square \Delta'$, the characteristic energy scale of the pinning mechanism operating in our thickness modulated films. In the thin film limit ($d << \lambda$) the potential energy $\varepsilon(\vec{r})$ of a vortex located at $\vec{r}$ can be expressed by the convolution[30] :

$$\varepsilon(\vec{r}) = \int f(\vec{r}' - \vec{r})\, d(\vec{r}')\, d^2r' \, , \tag{22}$$

where $d(\vec{r}') = d + \Delta d \cos qx$ is the periodically varying film thickness and $f(\vec{r}' - \vec{r})$ the free energy density distribution within the flux line. Using Clem's model[31] for $f(\vec{r}' - \vec{r})$, $\varepsilon(x)$ can be easily evaluated[10] from Eq. (22) in the limits $q\xi < 1$ (ξ is the GL-coherence length) and $q\Lambda >> 1$ of interest here. From the expression for $\varepsilon(x)$ one immediately identifies Δ as :

$$\Delta \approx 2n_\square (\Delta d/d)(\phi_o/4\pi)^2 \Lambda^{-1}(T) \, . \tag{23}$$

This result shows that Δ has the same temperature dependence as μ (Eq. 16), a considerable simplification in the analysis of the I_c-data. By combining Eqs. (21) and (23), I_{cM} can finally be written in the form :

$$\frac{I_{cM}(T)}{I_{cM}(0)} = \frac{\Lambda(0)}{\Lambda(T)} \left(\frac{\Delta}{\mu}\right)^{T/(T_{LU}-T)} , \qquad (24)$$

where $\Delta/\mu \approx 4(\Delta d/d)$. This expression shows very clearly how, with rising temperature, thermal fluctuations further reduce $I_{cM}(T)$ with respect to the BCS-value which corresponds to the limit $T_{LU} \to \infty$. After substraction of the background due to random pinning, which was deduced from a flat but otherwise identical reference film, the critical currents $I_{cM}(T)$ of *Al1* and *Al2* were fitted to Eq. (24) using $I_{cM}(0)$, Δ/μ and T_{LU}/T_c as fitting parameters. The result of this analysis is shown in Fig. 5 where, for comparison, theoretical curves calculated by neglecting the effect of thermal fluctuations are also shown. Good agreement with Eq. (24) is found for a reasonable choice of the parameters. T_{LU}/T_c scales with $R_{n\square}$

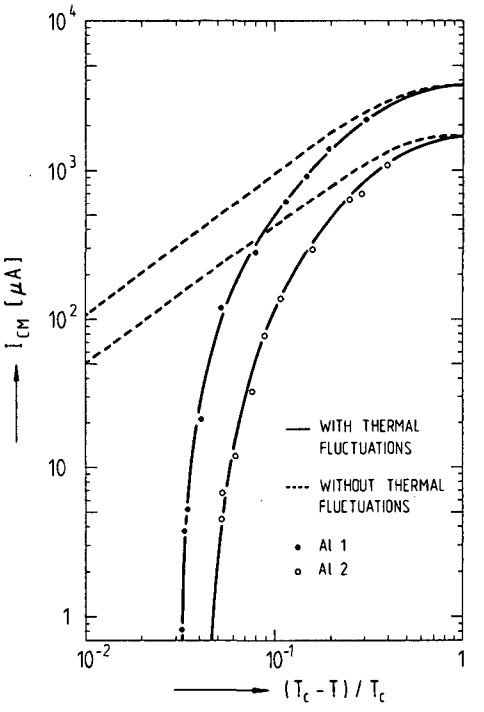

Fig. 5. Temperature dependence of the critical currents of thickness-modulated films in the perfectly registered ($\delta = 0$) C_{10}-phase. The experimental data are fitted to Eq. (24) using : $\Delta/\mu = 0.95$, $T_{LU}/T_c = 0.978$ for Al1 and $\Delta/\mu = 0.90$, $T_{LU}/T_c = 0.972$ for Al2.

approximately as predicted by Eq. (18) where, however, the numerical coefficient 0.31 is found to be about an order of magnitude too small to account for values deduced from the fit of Fig. 5. As for Δ/μ, there is good agreement between the values obtained from the fit and those estimated with $\Delta/\mu \approx 4(\Delta d/d)$ using the experimental data of $\Delta d/d$ listed in Table 1.

DYNAMICS

The motion of superconducting vortices in a periodic field shows interesting quantum features reminiscent of ac-Josephson phenomena in arrays of superconducting weak links. When the dc driving current I_{dc} exceeds I_c, a particular flux-flow régime characterizes a C-phase. Dynamic coupling of the vortex lattice with the periodic substrate results, in this case, in a highly coherent velocity oscillation of the vortices which, in turn, generates a weak but detectable macroscopic voltage oscillation[2,3], typically in the radiofrequency (rf) range. Indirect evidence for the collective oscillation of the vortices in a C-phase is obtained by exposing thickness-modulated films to rf-radiation. Pinning-induced coupling at rf-frequencies between the oscillating motion of the vortex lattice and the rf-field gives rise to quantum interference transitions in the I-V-curves at discrete values, $E_n = n\nu\lambda_g B$, of the flux-flow dc electric field E_{dc}[3,9,32] ($\nu = \Omega/2\pi$ is the frequency of the rf-radiation). Derivatives of the I-V-characteristics for Al*1* exposed to 100 MHz-radiation are shown in Fig. 6. As in the critical current case (Fig. 4), from the evolution of the n = 1 interference transition with increasing temperature one is led to the conclusion that dynamic coupling of the matched vortex lattice to the periodic substrate is totally absent for $T > T_{LU} \approx 1.85$ K. This provides additional evidence for the occurrence of the locking-unlocking phase transition discussed in the previous section. More detailed information about the dynamics of the 2D vortex lattice in the various phases it can assume on the periodic substrate can be obtained from a study of the complex rf-impedance of thickness-modulated layers. In the rest of this lecture we shall therefore focus our attention on some theoretical and experimental aspects of the dynamic response of the vortex medium to a small oscillating driving field.

Low Temperature Vortex Mobility

At low temperatures ($T << T_{LU}$) thermal fluctuations of the vortices can be neglected. Assuming a driving Lorentz force of the form $\vec{F}_L = d\phi_0(\vec{j}_{rf} \times \hat{z})\exp(-i\Omega t)$, the equation of motion for the position $\vec{r}_l$ of the vortex associated with the lattice site l can

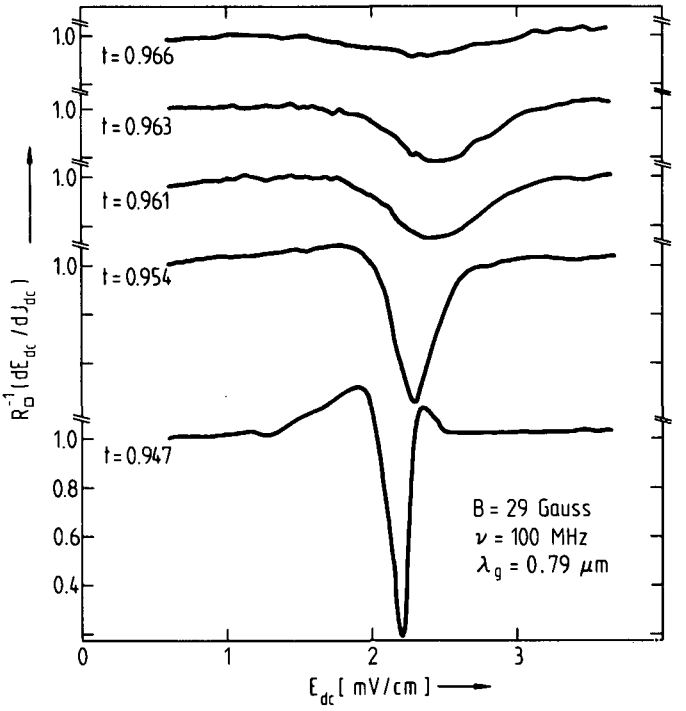

Fig. 6. Derivatives of the rf-excited current-voltage characteristics of Al1 showing the temperature dependence of the n = 1 interference transition.

then be written as[3] :

$$\eta \dot{\vec{r}}_{\underline{l}} = \vec{F}_L + \Delta' \vec{q} \sin \vec{q} \cdot (\vec{r}_{\underline{l}} - \vec{r}_o) - \sum_{\underline{l}'}{}' \frac{\partial W_{\underline{l}\underline{l}'}}{\partial r_{\underline{l}\underline{l}'}} \hat{r}_{\underline{l}\underline{l}'} , \qquad (25)$$

where $W_{\underline{l}\underline{l}'}$ is the interaction energy between the two vortices at $\vec{r}_{\underline{l}}$ and $\vec{r}_{\underline{l}'}$, $r_{\underline{l}\underline{l}'} = |\vec{r}_{\underline{l}} - \vec{r}_{\underline{l}'}|$ and $\vec{r}_o$ defines the relative position of the vortex lattice with respect to the 1D thickness modulation. Thus, the last term in Eq. (25) is the restoring force set up by the lattice in response to the periodic pinning force. To determine the linear response of the vortex medium to $\vec{F}_L$, one should study the oscillating motion of the vortices about their static equilibrium configuration characterized by the deformation field $\vec{w} = (u,v)$ described by Eq. (2). In the continuum limit this problem can be

solved exactly in terms of elliptic functions[33]. To avoid the rather complex algebra of this treatment, in this lecture we shall rely on a simpler perturbative approach which contains, however, all the essential physical features of the vortex dynamics. We assume that Δ is small and, consequently, write the solution of Eq. (25) in the form[3] :

$$\vec{r}_{\underline{l}} = \vec{\underline{l}} + i(\vec{v}_{rf}/\Omega)\, e^{-i\Omega t} + \vec{u}_{\underline{l}} \,, \tag{26}$$

where $\vec{v}_{rf} = (d\phi_o/\eta)(\vec{j}_{rf} \times \hat{z})$. The first two terms in Eq. (26) represent the solution of Eq. (25) in the flat-film case ($\Delta = 0$), whereas $\vec{u}_{\underline{l}}$ is the (small) additional dynamic displacement caused by the (weak) periodic pinning force. Substituting $\vec{r}_{\underline{l}}$, as given by Eq. (26), into Eq. (25) and expanding up to first order in the small quantities $\vec{q} \cdot \vec{u}_{\underline{l}} << 1$ and $(\vec{q} \cdot \vec{v}_{rf})/\Omega << 1$ one obtains :

$$\eta \dot{\vec{u}}_{\underline{l}} = - \sum_{\underline{l}'}{}' \tilde{G}(\underline{l} - \underline{l}')\vec{u}_{\underline{l}'} +$$

$$+ \frac{\Delta'}{2i} \sum_{\vec{q}} \vec{q}(1 + i\vec{q} \cdot \vec{u}_{\underline{l}}) \left(1 - \frac{\vec{q} \cdot \vec{v}_{rf}}{\Omega}\, e^{-i\Omega t}\right) e^{i\vec{q} \cdot (\vec{l} - \vec{r}_o)} \,, \tag{27}$$

where the sum in the last term is over $\vec{q}$ and $-\vec{q}$ (two terms). To solve Eq. (27) it is again convenient to expand $\vec{u}_{\underline{l}}$ in (transverse) normal modes of the lattice. The resulting expression contains terms proportional to the normal mode amplitudes $\vec{u}_t(\vec{k},\omega)$, $\vec{u}_t(\vec{k} \pm \vec{q},\omega)$ and $\vec{u}_t(\vec{k} \pm \vec{q},\ \omega \pm \Omega)$. Since we are interested in situations where $\vec{q}$ is close to one of the reciprocal lattice vectors $\vec{g}$ ($\vec{q} \approx \vec{g}$), one can set $\vec{u}_t(\vec{k} \pm \vec{q},\omega) \approx \vec{u}_t(\vec{k},\omega)$. Moreover, one can neglect, to a first approximation, terms involving $\vec{u}_t(\vec{k} \pm \vec{q},\omega \pm \Omega)$ which, arising from the product $(\vec{q} \cdot \vec{u}_{\underline{l}})(\vec{q} \cdot \vec{v}_{rf})/\Omega$ in Eq. (27), are small compared to those proportional to $\vec{u}_t(\vec{k},\omega)$. Then, the equation of motion can be solved for $\vec{u}_t(\vec{k},\omega)$ and the resulting expression is used to calculate the contributions, proportional to $\vec{u}_t(\vec{k} \pm \vec{q},\ \omega \pm \Omega)$, neglected in the first order approximation. Finally, a new solution, now accurate to second order in Δ, is worked out from which the vortex velocity $\vec{v}_{\underline{l}}(t) = \dot{\vec{r}}_{\underline{l}}$ is easily deduced. At this point, in order to describe the anisotropic dynamic response of the 2D vortex lattice in the 1D periodic potential, we introduce a vortex mobility tensor $\tilde{\mu}(\Omega)$ defined by $\vec{v}(\Omega) = \tilde{\mu}(\Omega)\vec{F}_L(\Omega)$, where $\vec{v}(\Omega)$ is the vector amplitude of the oscillating flux-flow velocity of the vortex medium. $\vec{v}(\Omega)$ follows by averaging $\vec{v}_{\underline{l}}(t)$ over all vortices of the lattice. An alternative way to describe the lattice response is in terms of a vortex impedance tensor $\tilde{Z}_{v\square}(\Omega)$ defined by $\vec{E}(\Omega) = \tilde{Z}_{v\square}(\Omega)\vec{J}(\Omega)$, where $\vec{E}(\Omega) = -\vec{v}(\Omega) \times \vec{B}$ and $\vec{J}(\Omega) = d\vec{j}(\Omega)$ are, respectively, the electric

field and sheet ($\square$) current amplitudes. Since in a coordinate system with the x-axis pointing in the $\vec{q}$-direction both $\tilde{\mu}(\Omega)$ and $\tilde{Z}_{v\square}(\Omega)$ are found to be diagonal, their components are simply related to each other by $Z_{v\square xx} = n_{\square}\,\phi_o^2\,\mu_{yy}$ and $Z_{v\square yy} = n_{\square}\,\phi_o^2\,\mu_{xx}$. Within our perturbative approach we find $\mu_{yy} = \eta^{-1}$, as expected, and :

$$\mu_{xx} = \eta^{-1}\left(1 - \frac{1}{2}\,\frac{1}{1 - i\Omega\tau}\,\delta_{\vec{q},\vec{g}} - \frac{1}{2}\,\frac{\Delta/\mu}{(1 - i\Omega\tau)\left[(b-1)^2 + (\Delta/\mu)\right]}\right) \qquad (28)$$

where $b = B/B_{mn}$ and $\tau = \eta/\Delta' q^2$ is the characteristic time for vortex relaxation in the potential wells. In writing the last term of Eq. (28) we have expressed the restoring force constant μk^2, where $\vec{k} = \vec{q} - \vec{g}$ is the wave vector of the pinning-induced shear deformation propagating at 45^o with respect to $\vec{q}$, in terms of b (or, alternatively, of δ) using the results of Ref. 3. Real and imaginary parts of μ_{xx} (or $Z_{v\square yy}$), as deduced from Eq. (28), are shown in Fig. 7 (dashed curves) as a function of b. There is a discontinuous jump in both components at $b = 1$ ($\delta = 0$). This reflects the onset of the CI-phase transition which, in our approximation, occurs for $\delta_c = 0$. In the exact calculation[33] both $\mathrm{Re}[Z_{v\square}]$ and $\mathrm{Im}[Z_{v\square}]$ are constant within a C-phase and equal to the corresponding values given by Eq.

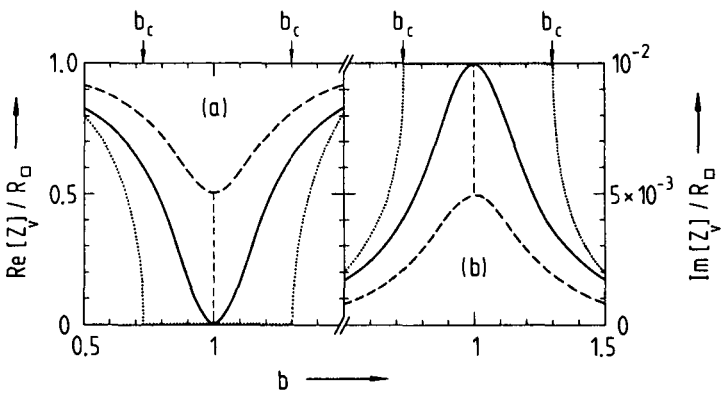

Fig. 7. Real (a) and imaginary (b) part of the normalized vortex impedance as a function of $b = B/B_{mn}$. The driving current flows in the y-direction perpendicular to $\vec{q}$. $\Delta/\mu = 0.05$, $\Omega\tau = 10^{-2}$. The significance of the various curves is explained in the text.

(28) for $b = 1$ ($\vec{q} = \vec{g}$) up to the critical mismatch δ_c (dotted curves in Fig. 7). One way to correct for the jump at $b = 1$ and to improve our approximation is to write μ_{xx} in the following form :

$$\mu_{xx} = \eta^{-1}\left(1 - \frac{\Delta/\mu}{(1 - i\Omega\tau)[(b-1)^2 + \Delta/\mu]}\right) \qquad (29)$$

As shown in Fig. 7 (full curves) this expression provides a reasonable description of the actual lattice response. For this reason we shall rely on Eq. (29) for the interpretation of the sheet conductance measurements reported in the last section of this lecture.

There is a simple physical interpretation for the general behaviour of $\mathrm{Re}[Z_{v\square}]$ and $\mathrm{Im}[Z_{v\square}]$ shown by Fig. 7. In a C-phase dissipation arises from the excitation, in the viscous vortex medium, of a collective mode in which the vortices oscillate in phase around their equilibrium positions at the bottom of the potential wells. In the I-phase additional dissipation results from the excitation of the soliton superstructure. Thus, $\mathrm{Re}[Z_{v\square}]$ must have its minimum value in a C-phase. $\mathrm{Im}[Z_{v\square}]$, on the other hand, measures the delay in lattice response caused by the periodic pinning structure. As the effect of pinning is strongest in a C-phase, $\mathrm{Im}[Z_{v\square}]$ is obviously largest in such a phase.

Sheet Conductance Measurements

To measure the dynamic response of the vortices in our thickness modulated layers, we rely on the two-coil experimental technique developed by Fiory and Hebard[34]. The superconducting film is mounted in a transverse plane between two coaxial closely-spaced coils, one (drive coil) providing the rf-excitation of the vortex medium, the other (receive coil) to detect its rf-response. For an isotropic 2D superconductor, as it is the case for a flat ($\Delta = 0$) superconducting film, Fiory and Hebard have shown that, in the limit of weak screening, the rf-voltage amplitude $V_R(\Omega)$ at the receive coil due solely to the rf-response currents flowing in the sample is proportional to $\Omega^2 G_\square I_D(\Omega)$, where $G_\square = Z_\square^{-1}$ is the (complex) sheet conductance of the film and $I_D(\Omega)$ the (constant) amplitude of the rf-current in the drive coil. A straightforward extension of this calculation to our anisotropic samples shows that, in the same weak-screening limit, $V_R(\Omega)$ can be written in the form :

$$V_R(\Omega) = \Omega^2 I_D(\Omega)(K_1 G_{\square xx} + K_2 G_{\square yy}) , \qquad (30)$$

where K_1 and K_2 are constants depending on the geometry of the

sample and of the two-coil configuration and the x-axis is still pointing in the $\vec{q}$-direction. According to Fiory and Hebard[35 36], $\tilde{Z}_{\square} = \tilde{G}_{\square}^{-1}$ can be expressed as a series connection of the vortex impedance $\tilde{Z}_{v\square}$ with the kinetic inductance $L_k = (1/2)\mu_0\Lambda$ associated with the superfluid background. Thus, using the results of the previous section, $Z_{\square xx} = G_{\square xx}^{-1} = (n_{\square}\phi_0^2/\eta) + i\Omega L_k$ and $Z_{\square yy} = G_{\square yy}^{-1} = n_{\square}\phi_0^2\mu_{xx} + i\Omega L_k$, where μ_{xx} is given by Eq. (29). Using typical parameters for our Al-films (Table 1), it can be easily verified that, except very close to T_c or at extremely low magnetic fields, the kinetic inductance term is always much smaller than the vortex impedance and can therefore be neglected in the analysis of most of our experimental data. Furthermore, in the vicinity of a registered phase ($B \approx B_{mn}$), the lattice configuration of interest here, $Z_{\square xx} \approx n_{\square}\phi_0^2/\eta$ varies weakly with B, while, on the contrary, $Z_{\square yy} \approx n_{\square}\phi_0^2\mu_{xx}$ shows pronounced structures (Fig. 7). Thus, if one uses a modulation technique, in which B is weakly modulated

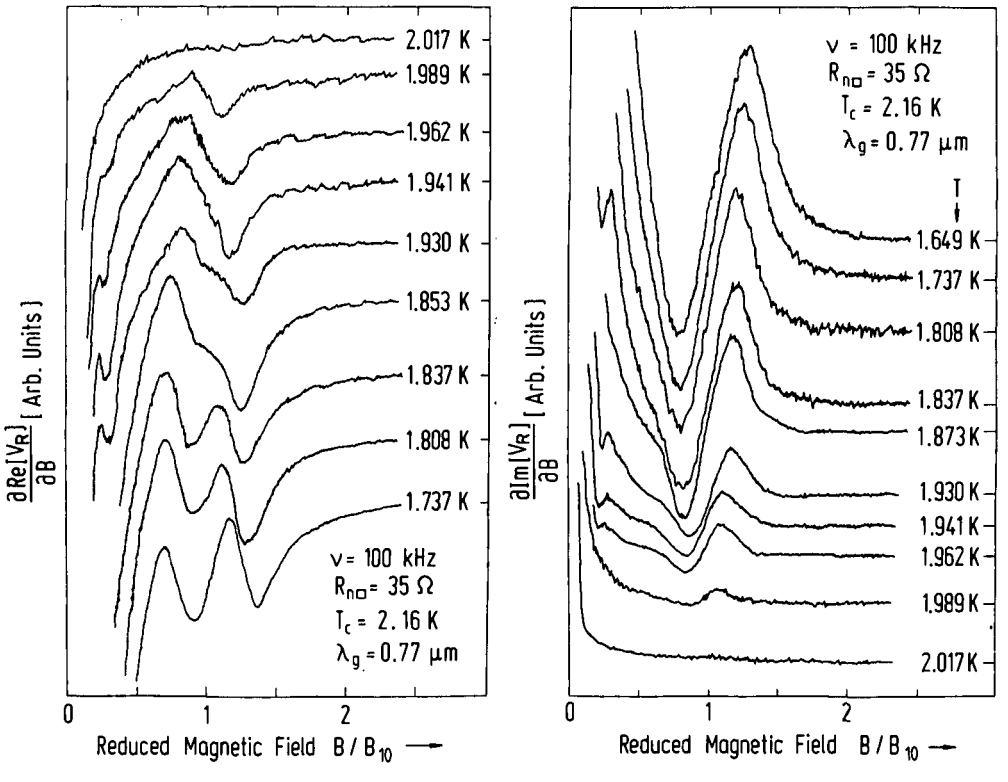

Fig. 8. Derivative curves of the in-phase and out-of phase components of the rf-response of Al2 as a function of B. Marks on the vertical axis denote the zero-level of the signal.

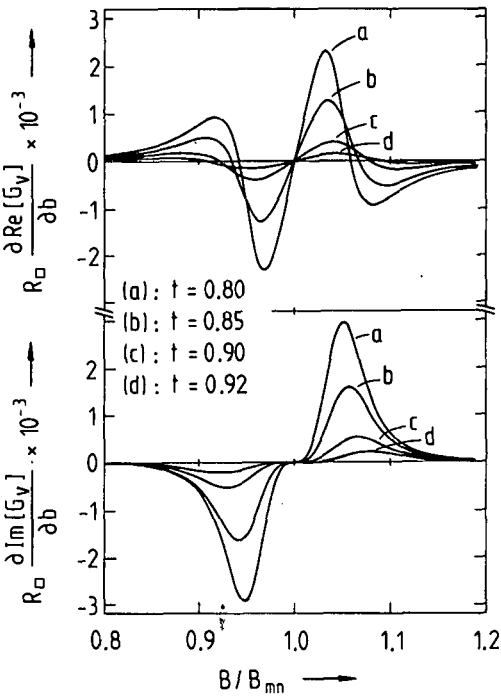

Fig. 9. Theoretical derivative curves of the complex vortex impedance for Al2 as deduced from Eqs. (29) and (14) using $\Delta/\mu = 0.9$. See text for the determination of $\Omega\tau(T)$.

($\delta B \approx 0.1$ Gauss) at a low frequency ($\sim$ 2 Hz), the signal one actually detects at the receive coil will be essentially proportional, for $B \approx B_{mn}$, to $\partial G_{\square yy}/\partial B$. In Fig. 8 sets of curves at different temperatures for the in-phase and out-of-phase components of the 100 kHz-signal for Al2, measured with a conventional phase-sensitive technique, are shown as a function of B. There are pronounced structures in both the real and imaginary parts in the vicinity of $B_{10} \approx 30$ Gauss (weaker structures are visible also in correspondence of the unresolved C_{11}- and C_{20}-phases). The shape of these structures should now be compared with that predicted by Eq. (29). To this purpose, in Fig. 9 we show theoretical curves calculated from Eq. (29) where, in an attempt to partially include the effect of thermal fluctuations, Δ/μ was replaced by Δ_R/μ and $\tau = \eta/\Delta_R' q^2 = \eta/q\phi_0 dj_{cM}$ [Eq. (20)] was estimated using the j_{cM}-data for Al2 of Fig. 5. While there is good qualitative agreement for both components of the signal at low temperatures, the evolution of the

structures about B_{10} with rising temperature is quite different from that predicted by Eq. (29). In particular, as one expects from the temperature dependence of the critical mismatch δ_c tolerated by a C-phase, their width becomes narrower and narrower as T approaches T_{LU}, a feature which does not emerge from the theoretical curves of Fig. 9. Clearly, a more elaborated model which takes into account, in particular, diffusion phenomena of "corrugated" domain walls should be worked out in order to describe the dynamic response of the periodically pinned 2D vortex lattice at high temperatures ($T \lesssim T_{LU}$). This, as well as the study of other features of the rf-response (in particular of the origin of the drastic crossover in response at low magnetic fields in Fig. 8) will be the object of future research in our laboratory.

ACKNOWLEDGEMENTS

We would like to thank J.R. Clem, V.L. Pokrovsky and M. Puga for stimulating discussions. This work has been supported by the Swiss National Science Foundation.

REFERENCES

1. O. Daldini, P. Martinoli, J. L. Olsen, and G. Berner, Vortex-line pinning by thickness modulation of superconducting films, Phys. Rev. Lett. 32:218 (1974).
2. P. Martinoli, O. Daldini, C. Leemann, and B. Van den Brandt, Josephson oscillation of a moving vortex lattice, Phys. Rev. Lett. 36:382 (1976).
3. P. Martinoli, Static and dynamic interaction of superconducting vortices with a periodic pinning potential, Phys. Rev. B 17:1175 (1978).
4. P. Bak, Commensurate phases, incommensurate phases and the devil's staircase, Rep. Prog. Phys. 45:587 (1982).
5. J. Villain, Theories of commensurate-incommensurate transitions on surfaces, in: "Ordering in two dimensions", S. K. Sinha, ed., North Holland, Inc., New York (1980).
6. J. M. Kosterlitz, and D. J. Thouless, Ordering, metastability and phase transitions in two-dimensional systems, J. Phys. C 6:1181 (1973).
7. D. R. Nelson, and B. I. Halperin, Dislocation-mediated melting in two dimensions, Phys. Rev. B 19:2457 (1979).
8. V. L. Pokrovsky, and A. L. Talapov, The theory of two-dimensional incommensurate crystals, Zh. Eksp. Teor. Fiz. 78:269 (1980) [Sov. Phys. JETP 51:134 (1980)].

9. P. Martinoli, H. Beck, M. Nsabimana, and G.-A. Racine, Locking-unlocking transition of a two-dimensional lattice of superconducting vortices, Physica 107B:455 (1981).
10. P. Martinoli, M. Nsabimana, G.-A. Racine, H. Beck, and J. R. Clem, Locked and unlocked phases of a two-dimensional lattice of superconducting vortices, Helv. Phys. Acta 55:655 (1982).
11. A. T. Fiory, Measurements of the shear modulus of the superconducting mixed state of thin films, Phys. Rev. B 8:5039 (1973).
12. F. C. Frank, and J. H. van der Merwe, One-dimensional dislocations, Proc. Roy. Soc. (London) A198:205 (1949).
13. J. Bardeen, and M. J. Stephen, Theory of the motion of vortices in superconductors, Phys. Rev. 140A:1197 (1965).
14. M. Tinkham, in: "Introduction to superconductivity", McGraw-Hill, Inc., New York (1975).
15. M. W. Puga, E. Simanek, and H. Beck, Renormalization-group approach to commensurate-incommensurate transitions in two dimensions, Phys. Rev. B 26:2673 (1982).
16. M. W. Puga, E. Simanek, and H. Beck, Commensurate-incommensurate transitions, to appear in Helv. Phys. Acta (1983).
17. B. A. Huberman, and S. Doniach, Melting of two-dimensional vortex lattices, Phys. Rev. Lett. 43:950 (1979).
18. D. S. Fisher, Flux-lattice melting in thin-film superconductors, Phys. Rev. B 22:1190 (1980).
19. J. V. José, L. P. Kadanoff, S. Kirkpatrick, and D. R. Nelson, Renormalization, vortices, and symmetry-breaking perturbations in the two-dimensional planar model, Phys. Rev. B 16:1217 (1977) [Erratum, Phys. Rev. B 17:1477 (1978)].
20. S. Ostlund, Relation between lattice and continuum theories of two-dimensional solids, Phys. Rev. B 23:2235 (1981).
21. S. Ostlund, Incommensurate and commensurate phases in asymmetric clock models, Phys. Rev. B 24:398 (1981).
22. J. Villain, and P. Bak, Two-dimensional Ising model with competing interactions : floating phase, walls and dislocations, J. Physique 42:657 (1981).
23. S. N. Coppersmith, D. S. Fisher, B. I. Halperin, P. A. Lee, and W. F. Brinkman, Dislocations and the commensurate-incommensurate transition in two dimensions, Phys. Rev. Lett. 46:549 (1981).
24. T. Bohr, V. L. Pokrovsky, and A. L. Talapov, Commensurate-incommensurate phase transition in continuous media containing dislocations, Pis'ma Zh. Eksp. Teor. Fiz. 35:165 (1982) [Sov. Phys. JETP Lett. 35:203 (1982)].
25. T. Bohr, Dislocations in the commensurate-incommensurate transition, Phys. Rev. B 25:6981 (1982).

26. F. D. M. Haldane, P. Bak, and T. Bohr, Phase diagramms of surface structures from Bethe-Ansatz solutions of the quantum sine-Gordon model, preprint (1982).
27. S. E. Burkov, and V. L. Pokrovsky, Critical currents and electric fields of two-dimensional systems, J. Low Temp. Phys. 44:423 (1981).
28. P. Martinoli, J. L. Olsen, and J. R. Clem, Superconducting vortices in periodic pinning structures, J. Less-Common Metals 62:315 (1978).
29. P. Martinoli, and J. R. Clem, Pinning in periodic superconducting structures, in: "Inhomogeneous superconductors-1979", D. U. Gubser, T. L. Francavilla, S. A. Wolf, and J. R. Leibowitz, ed., American Institute of Physics, New York (1980).
30. A. Schmid, and W. Hauger, On the theory of vortex motion in an inhomogeneous superconducting film, J. Low Temp. Phys. 11:667 (1973).
31. J. R. Clem, Simple model for the vortex core in a type II superconductor, J. Low Temp. Phys. 18:427 (1975).
32. P. Martinoli, O. Daldini, C. Leemann, and E. Stocker, A. C. quantum interference in superconducting films with periodically modulated thickness, Solid State Comm. 17:205 (1975).
33. V. L. Pokrovsky, private communication.
34. A. T. Fiory, and A. F. Hebard, Radio-frequency complex-impedance measurements on thin film two-dimensional superconductors, in: "Inhomogeneous superconductors-1979", D. V. Gubser, T. L. Francavilla, S. A. Wolf, and J. R. Leibowitz, ed., American Institute of Physics, New York (1980).
35. A. F. Hebard, and A. T. Fiory, Recent experimental results on vortex processes in thin-film superconductors, in: "Ordering in two dimensions", S. K. Sinha, ed., North Holland, Inc., New York (1980).
36. A. F. Hebard, and A. T. Fiory, Vortex dynamics in two-dimensional superconductors, Physica 109 & 110 B:1637 (1982).

LISTE DES PUBLICATIONS

/01/ *P. MARTINOLI, M. NSABIMANA*
Experiments on vortex lattice melting in thickness modulated superconducting films.
Helv. Phys. Acta 53 : 606 (1980).

/02/ *H. BECK, E. SIMANEK, M.PUGA, P. MARTINOLI, M. NSABIMANA, G.-A. RACINE*
Statics and dynamics of the vortex lattice in a modulated superconducting film.
Helv. Phys. Acta 54 : 651 (1981).

/03/ *P. MARTINOLI, H. BECK, M. NSABIMANA, G.-A. RACINE*
Locking-unlocking transition of a two-dimensional lattice of superconducting vortices.
Physica. 107 B : 455 (1981).

/04/ *M. NSABIMANA, G.-A. RACINE, H. BECK and P. MARTINOLI*
Complex impendance measurements of superconducting films at RF - frequencies.
Helv. Phys. Acta 54 : 272 (1981).

/05/ *P. MARTINOLI, M. NSABIMANA, H. BECK, and M. PUGA*
Dynamics of the melting transition of a two-dimensional lattice of superconducting vortices.
Helv. Phys. Acta 55 : 550 (1982).

/06/ *P. MARTINOLI, M. NSABIMANA, G.-A. RACINE, H.BECK and J.R. CLEM*
Locked and unlocked phases of a two-dimensional lattice of superconducting vortices.
Helv. Phys. Acta 55 : 655 (1982).

/07/ *P. MARTINOLI, M. NSABIMANA, G.-A. RACINE, H. BECK and J.R. CLEM*
Search for two-dimensional melting in a lattice of superconducting vortices.
Helv. Phys. Acta 56 : 765 (1983)

/08/ *P. MARTINOLI, H. BECK, M. NSABIMANA and G.-A. RACINE*
Static and Dynamic properties of Commensurate and Incommensurate phases of a two-dimmensional lattice of superconducting films.
To appear in NATO Advanced Study Institute on "Percolation, Localization and Superconductivity". Les Arcs, june 1983, A.M. Goldman and S.A. Wolf ed. Plenum Press, New York (1983).

/09/ *H. BECK, Ph. RENAUD, P. MARTINOLI, M. NSABIMANA and M. PUGA*
Dynamics of melting in 2-d lattice.
To appear in Helv.Phys. Acta 56 : (1983).

/10/ *P. MARTINOLI, M. NSABIMANA, G.-A. RACINE and H. BECK*
Dynamique de phases Commensurables et Incommensurables du réseau de vortex supraconducteurs.
Bulletin de la Société Française de Physique, supplément au No 49 : 22 (B-32) 1983.

- - - - - - -